DETERMINATIONS OF MAJOR IONS IN ULUDAĞ NATIONAL PARK

A THESIS SUBMITTED TO THE GRADUATE SCHOOL OF EDUCATION
FACULTY
OF
THE MIDDLE EAST TECHNICAL UNIVERSITY

BY

SERPİL (YENİSOY) KARAKAŞ

IN PARTIAL FULFILMENT OF THE REQUIREMENTS FOR THE DEGREE
OF
MASTER OF SCIENCE
IN
THE DEPARTMENT OF SCIENCE EDUCATION

APRIL 1995

To my parents and my husband

Approval of the Graduate School of Education Faculty

Prof. Dr. İsmail TOSUN
for
Director

I certify that this thesis satisfies all the requirements as a thesis for the degree of Master of Science.

Prof. Dr. İlker Özkan
Head of Department

This is to certify that we have read this thesis and that in our opinion it is fully adequate, in scope and quality, as a thesis for the degree of Master of Science.

Assoc.Prof. Semra G. Tuncel
Supervisor

Examining Comittee Members

Prof. Dr. Namık K. Aras (Chairman)
Assoc. Prof. Semra G. Tuncel
Prof Dr. Ahmet Önal
Prof. Dr. Gürdal Tuncel
Assoc. Prof. Şahinde Demirci

ABSTRACT

DETERMINATIONS OF MAJOR IONS IN ULUDAĞ NATIONAL PARK

KARAKAŞ (YENİSOY), Serpil

M.S., Department of Science Education

Supervisor: Assoc. Prof. Semra G. Tuncel

April 1995, 114 pages

Major ions in aerosol and snow samples in Sarıalan region of Uludağ National Park were determined. One hundred eighty four aerosol samples were collected daily during the period of September 1993-March 1994 and nine snow samples were collected weekly during the period of December 1993-April 1994. The composition of the samples were determined by using flame Atomic Absorption Spectrometer for Na^+, K^+, Mg^{2+} and Ca^{2+}, Ion Chromatography for Cl^-, NO_3^-, SO_4^{2-} and Colorimetry for NH_4^+.

Sulfate made up 30 % of aerosol mass and concentrations of ions except Ca^{2+} in aerosol were comparable with the literature values. Calcium, Mg^{2+}, K^+ and Na^+ ions were mostly originated from crustal contribution

however Mg^{2+}, Na^{+} and Cl^{-} were also affected by marine source which is about 30 km north (Marmara Sea) of the sampling site. The concentration of sulfate was maximum in autumn and the concentration of nitrate was maximum in spring. Photochemical conversion of SO_2 to SO_4^{2-} was significant in autumn. Acid causing anions SO_4^{2-} and NO_3^{-} were not strongly related to Ca^{2+}, Mg^{2+} and NH_4^{+} implying that they were mostly in the form of H_2SO_4 and HNO_3 in aerosol samples. Wind sector analysis showed that although the sources located at north have the same pollution strength as the sources located at south, southerly winds made the greatest contribution to all parameters because of high frequency of winds from this sector. Northerly winds carries the plumes of urban, industrial emissions and marine aerosols whereas southerly winds carries the plumes of a power plant and ski resort area.

Concentrations of ions in snow involved both dry and wet deposition. The strong acids H_2SO_4 and HNO_3 were neutralized by NH_3 and basic cations. However pH of snow samples showed an acidic character since organic acids which are released from trees are effective species in both aerosol and snow composition. This can also be inferred from the observed anion deficiency in both samples since organic anions were not analyzed.

Keywords: Aerosol, snow, rural, wind sector analysis, major ions, organic acids.

ÖZ

ULUDAĞ MİLLİ PARKINDA TEMEL İYONLARIN BELİRLENMESİ

KARAKAŞ (YENİSOY), Serpil

Yüksek Lisans Tezi, Fen Bilimleri Eğitimi Bölümü

Tez Yöneticisi: Assoc. Prof. Semra G. Tuncel

Nisan 1995, 114 sayfa

Bu çalışma da, Uludağ Milli Parkı'nın Sarıalan bölgesinde toplanan aerosol ve kar örneklerinde temel iyonların belirlenmesi yapılmıştır. Yüz seksen dört aerosol örneği Eylül 1993 ile Mart 1994 arasında günlük toplanmıştır ve dokuz kar örneği Aralık 1993 ile Nisan 1994 tarihleri arasında haftalık toplanmıştır. Örneklerin kompozisyonu Cl^-, NO_3^- ve SO_4^{2-} için İyon Kromatografisi, Na^+, K^+, Mg^{2+} ve Ca^{2+} için Atomik Absorsiyon Spektrometrisi ve NH_4^+ için Kolorimetre kullanılarak bulunmuştur.

Sulfatın aerosol kütlesinin % 30'unu oluşturduğu ve kalsiyum hariç diğer iyonların konsantrasyonlarının literatür değerleri ile karşılaştırılacak

düzeyde olduğu görülmüştür. Kalsiyum, Mg^{2+}, K^{+} ve Na^{+} iyonları daha çok yer kabuğundan gelmiştir. Öte yandan Mg^{2+}, Na^{+} ve Cl^{-} miktarları örnekleme yerinin 30 km kuzeyinde bulunan Marmara denizinden etkilenmiştir. Sulfat konsantrasyonu sonbaharda en yüksek, nitrat konsantrasyonu ise ilkbaharda en yüksektir. Kükürt dioksitin sülfata fotokimyasal dönüşümü sonbaharda etkili olmuştur. Asit iyonları olan SO_4^{2-} ve NO_3^{-} ın Ca^{2+}, Mg^{2+} ve NH_4^{+} ile çok kuvvetli bir ilişki göstermemesi onların aerosol örneklerinde H_2SO_4 ve HNO_3 formunda olduklarını ifade etmektedir. Rüzgar sektörü analizi göstermiştir ki, kuzey rüzgarları, güney rüzgarları kadar kirletme gücüne sahip olmalarına rağmen, güney rüzgarları, rüzgarın esme frekansının bu yönden fazla olmasından dolayı, en büyük katkıyı yapmıştır. Kuzey rüzgarları şehir, endüstri ve deniz aerosollarını taşırken, güney rüzgarları termik santral ve kayak merkezinin kirleticilerini taşımaktadır.

Kardaki iyon konsantrasyonları da, kuru ve yaş çökelme toplamından oluşmaktadır. Kuvvetli asitler olan H_2SO_4 ve HNO_3, NH_3 ve bazik katyonlar tarafından nötürlenmişlerdir. Fakat kar örneklerinin pH'ı asidik karakterdedir bu da ağaçlardan gelen organik asitlerin aerosol ve kar kompozisyonunda etkili olmasındandır. Bu durum her iki örnekde de organik iyonların analiz edilmemesinden gelen anyon eksikliğinden anlaşılmaktadır.

Anahtar Kelimeler: Aerosol, kar, kırsal, rüzgar sektörü analizi, temel iyonlar, organik asitler.

ACKNOWLEDGEMENTS

I would like to express my sincere appreciation to my supervisor Assoc. Prof. Semra G. Tuncel for her encouragement, quidance and kind suggestions throughout this study.

I would like to thank Prof. Dr. Gürdal Tuncel for his suggestions and his help to make the instruments available for me in the Environmental Engineering Department.

I also thank to Prof. Dr. Ulviye Özer for her help for supplying the necessary equipment to do sampling during the sampling period.

Kind helps of technician Ayfer Esen from Department of Environmental Engineering for the supplying the necessary equipments for my experiments was also valuable.

My special thanks to my fellow graduate students in the Environmental Analytical Group, Mustafa Yatın, Idrees Al-Momani, Güven Kaya, Müge Önal and Soner Erduran for their moral support and friendly help of teaching computer programs and endless suggestions of especially

senior group members. My special thanks goes to Idrees Al-Momani, Güven Kaya and Turan Karakaş for their help in the analysis of samples by AAS.

And, my special thanks are for my husband Turan Karakaş for his moral support and willingness to endure with me in the Chemistry Department in the late evenings during the writing of this thesis.

TABLE OF CONTENTS

LIST OF TABLES

Pages

TABLE

LIST OF FIGURES

Pages

FIGURES

CHAPTER I

INTRODUCTION

1.1 An overview of air pollution

Air pollutants are substances which, adversely affect the humans, animals, plants, or microbial life, damage materials, or interfere with the enjoyment of life and the use of property. The increasing demand for energy generation in all forms lies at the root of the air pollution problem because of uncontrolled emissions.

A global picture of pollutants from source to receptor is summarized in Figure 1.1 [1]. Primary pollutants are defined as the ones which are emitted directly into the atmosphere from their sources; for example, SO_2, NO_x, CO, Pb, organics, and particulate matter. Once in the atmosphere, they are subjected to dispersion and transport, that is meteorology, and simultaneously to chemical and physical transformations into gaseous and particulate secondary pollutants, defined as those formed from reactions of the primary pollutants in the air such as ozone. The pollutants may be removed at the earth's surface via wet or dry deposition and can impact a variety of receptors such as, humans, animals, aquatic ecosystems, vegetation, and materials. From a detailed knowledge of the emissions, topography, meteorology, and chemistry, one can develop mathematical

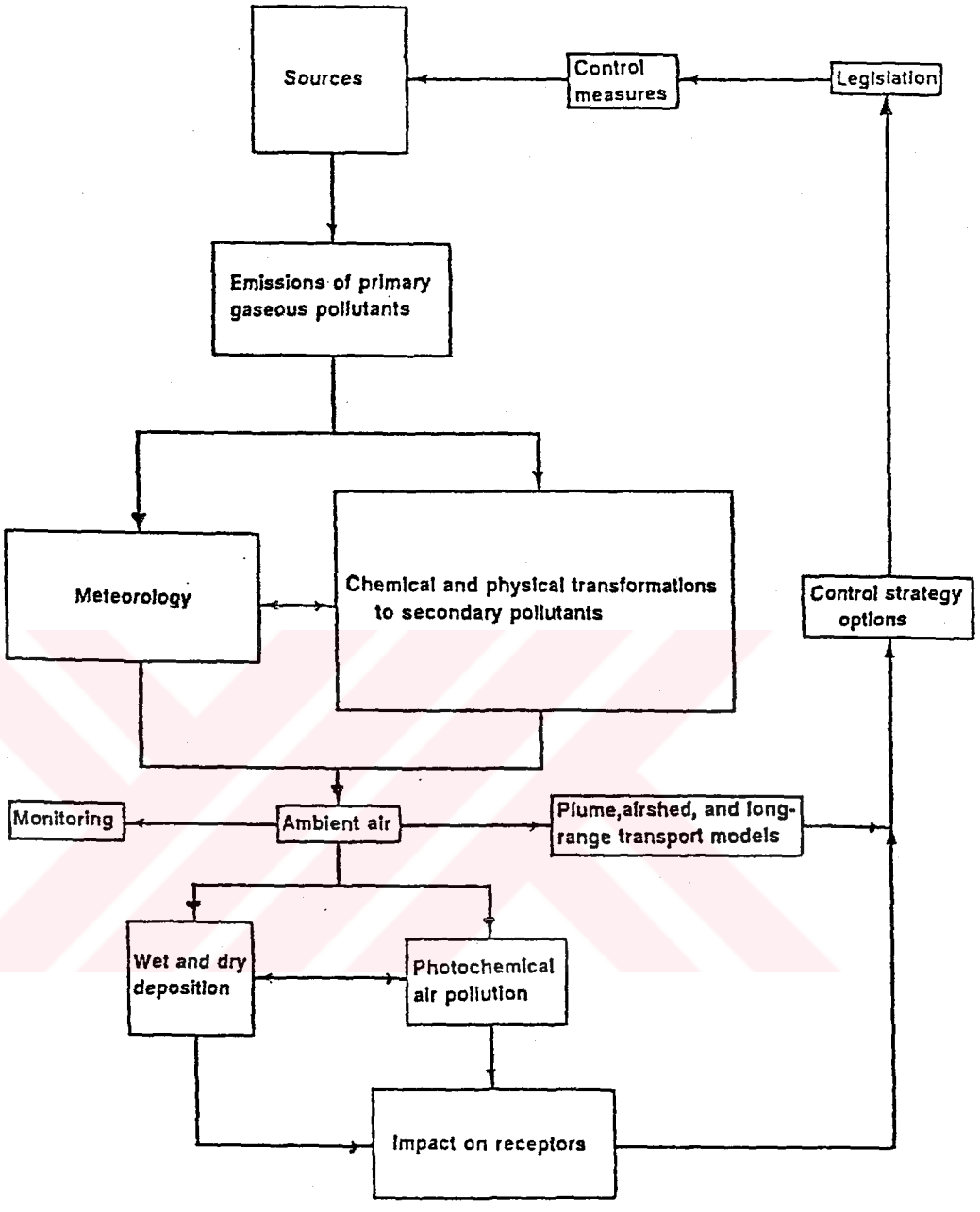

Figure 1.1 The air pollution system

models that predict the concentrations of primary and secondary pollutants as a function of time at various locations in a given airshed. In order to verify these models, these predictions must be compared to concentrations measured in ambient air monitoring programs. Then, various control strategies are developed and finally through legislative and administrative action, control measures can be formulated. Control measures may affect our air pollution system, that is the primary emissions and their sources.

As shown in the Table 1.1, there are various of natural and man-made source of air pollutants.

Table 1.1. Major sources of air pollutants.

Natural	Man-made
Volcanoes	Combustion generated pollutants
Biological activities	Emission from engines
Sea spray	Non-combustion sources
Pollens, terpenes	(Gases, dusts, odours)
Blowing dust	

Natural Emissions

Within a local area the levels of most pollutants are usually dominated by the man-made contributions. However, nature is also a generator of pollutants and on a global scale the natural emissions far outweigh human emissions [2]. Sulfur, in the form of SO_2, is emitted most dramatically from volcanoes: globally this may amount to $5*10^6$ tons S/yr.

However, larger amounts are emitted within sea spray (as sulfate $44*10^6$ tons/yr) and from biological processes. In the absence of air, biological decay results in emissions of H_2S and organic sulfur compounds such as dimethyl sulfide. Together these may contribute up to $100*10^6$ tons/yr. Since the global SO_2 from combustion emissions is also approaching $100*10^6$ tons S/yr, the natural and anthropogenic sulfur emissions are comparable. The grouping together of all sulfur compounds is appropriate since H_2S and organic sulfur compounds are converted into SO_2 in the atmosphere.

Biological processes in soil lead to the release of all of the common nitrogen oxides, NO, NO_2, and N_2O. The amounts involved are uncertain but are of the hundred million tons per year. In comparison, the anthropogenic emissions of NO and NO_2 from combustion are 50 million tons per year and for N_2O essentially zero (unless we include N_2O derived from soil action on nitrogenous fertilizers). A similar situation applies for NH_3, the other nitrogen containing gas. Anthropogenic emissions are only a few million tons per year, mainly from waste treatment. Natural emissions from biological decay and animal excrement exceed 100 million tons per year although, again, the exact amount is highly uncertain.

The major natural source of hydrocarbons is the generation of methane from biological decay. Heavier hydrocarbons, such as terpenes, are released directly to the atmosphere from trees. Global emissions considerably exceed anthropogenic emissions.

Man-made Emissions

Combustion sources are the major contributor to the man-made emissions. The main elemental components of fossil fuels are carbon and hydrogen. When burnt with the oxygen present in air, CO_2 and H_2O are released. Carbon dioxide is harmless to man, being a natural product of our metabolic processes which is exhaled in our breath. The concern over its wider role in the atmosphere and its possible effect on climate through green-house effect. The water vapour emitted by human activities is generally negligible compared with the water vapour naturally present in the atmosphere. In a flame the hydrocarbon fuel molecules are progressively broken down to smaller fragments and combine with oxygen. The end product of this stage of the reaction is carbon monoxide. Soot formation commonly accompanies carbon monoxide formation and is again generally due to inadequate air supply. The resultant soot particles are commonly sub-micron (< 1 μm) and because they are of comparable size to the wavelength of light they are effective both in light absorption and light scattering.

Sulfur dioxide arises from sulfur present in most fuels. In coal this takes the form partly of mineral matter pyrites (FeS_2) and partly of organic sulfur compounds. A small fraction of the SO_2, usually less than 1 %, may be further oxidized to SO_3, which combines with water vapour to form H_2SO_4 in the flue gas. There are two main routes to the formation of nitrogen oxides. One involves the combination of nitrogen and oxygen in the air at the peak flame temperatures to form NO. The other starts with the nitrogen originally present in the fuel. In addition to SO_2 and NO, the combustion of coal produces HCl, originating from chlorides in the fuel at a level 0.2 % by weight. Although not generally considered to be as

an important contributor to pollution problems, it adds to the acidity of precipitation.

1.2. Behaviour of Pollutants in The Lower Atmosphere

The processes which need to be considered between the emission of pollutants and their eventual destruction or removal to the ground are their dispersion (e.g. by winds), transportation and transformation. We will concentrate on chemical transformation rather than transportation and dispersion. The chemical processes involved are complex and different in the gas, aqueous and solid phases. Not only do we have to consider the transformations of the primary pollutants but also the formation of secondary pollutants which can have adverse effects on the environment and on human health [2].

1.2.1. Gases

Photons of ultraviolet light provide a means of initiating chemical reactions that would otherwise not take place. Most photochemical reactions starts with free radicals such as hydroxyl $OH\cdot$, hydroperoxly $HO_2\cdot$, and methyl $CH_3\cdot$ [3]. Free radicals are extremely reactive and have very short lifetimes. Concentrations in the atmosphere are small but not negligible. For the common inorganic pollutants like oxides of nitrogen and sulfur the overall result is the formation of nitric acid and sulfuric acid formation.

$$NO, NO_2 \rightarrow HNO_3$$

$$SO_2 \rightarrow H_2SO_4$$

The main species initiating the sequence of reactions is the hydroxyl radical:

$$NO_2 + OH\cdot \rightarrow HNO_3$$

$$SO_2 + OH\cdot \rightarrow HSO_3\cdot$$

In the case of nitric acid formation , there are no remaining free radicals to continue the chain of reactions. The oxidation rate of SO_2 can be 2 % h^{-1} in urban air or a factor of 10 lower in clean air, resulting in an overall lifetime of a few days. Radicals other than $OH\cdot$, such as $HO_2\cdot$, $CH_3O_2\cdot$ or other hydrocarbon peroxy radicals will also attack SO_2 but at a lower rate and their contribution to the overall oxidation is thought to be relatively small.

$$HSO_3\cdot + O_2 \rightarrow SO_3 + HO_2\cdot$$

$$SO_3 + H_2O \rightarrow H_2SO_4$$

1.2.2. Particulate Matter (Aerosol)

Aerosols are defined as relatively stable suspensions of solid or liquid particles in a gas phase such as smoke, fog or mist [4]. Particles and particulates are used interchangeably with aerosols. They may have diameters between ~ 0.002 μm and ~100 μm.

The nitric acid and sulfuric acid in the gas reactions generally undergo further changes. They both are water soluble and will be rapidly

absorbed by water droplets. They may react with solid particles forming sulfates and nitrates. For example $CaCO_3$ can be converted into $CaSO_4$ and salt particles (NaCl), perhaps of marine origin, can be converted into Na_2SO_4 or $NaNO_3$. However, the most common are those involving ammonia. The fate of NH_3 emissions into the atmosphere is illustrated in Figure 1.2. Here it is important to distinguish carefully between what remains as gaseous NH_3, and what is transformed into NH_4^+ ions in association with SO_4^{2-}, NO_3^- and Cl^- ions [5]. Close to the ground over an area emitting NH_3 there is a competitive effect of upwards diffusion by atmospheric turbulence and redeposition downwind over areas of lower ground concentration. Moreover the upward fluxes of NH_3 are depleted by conversion to NH_4^+ ions by reaction with acidic species that is ammonia reacts with HNO_3 vapor. The rate of conversion of NH_3 into NH_4^+ in this way as NH_3 diffuses upwards clearly depends on the concentration of the acidic species. In addition to this reactions with OH radicals also reduce NH_3 concentrations but only at an insignificant rate. Ammonia penetrating up to cloud level neutralizes SO_2 or NO_x within cloud droplets. Clouds are continually forming and evaporating resulting in particulates or precipitation and particulate or gaseous ammonia may be removed from the atmosphere by wet or dry deposition. The largest source of ammonia is thought to be animal discharge and fertilizers [2].

Particles formed by gaseous reactions are initially very small (<0.1 μm) but grow rapidly either by surface accumulation of material from the gas or by particle-particle coagulation [2]. Once in the size range 0.1-2.0 μm, they become relatively stable towards further growth and can remain airborne for periods of days. Most smoke emissions are in this category, along with the sulfates and nitrates. At the other end of the size spectrum

(2-50 μm) is coarse dust, and sea salt left from the evaporation of spray is also coarse. The larger the particles, the more rapidly they fall out of the air under the influence of gravity. Particles larger than 150 μm diameter, falling at over 1 m s^{-1} , remain airborne for such a short time that they do not need to concern us as air pollutants. Particles less than 5 μm have sedimentation velocities that are so low that their movement is determined by the natural turbulence of the air, just as for gases.

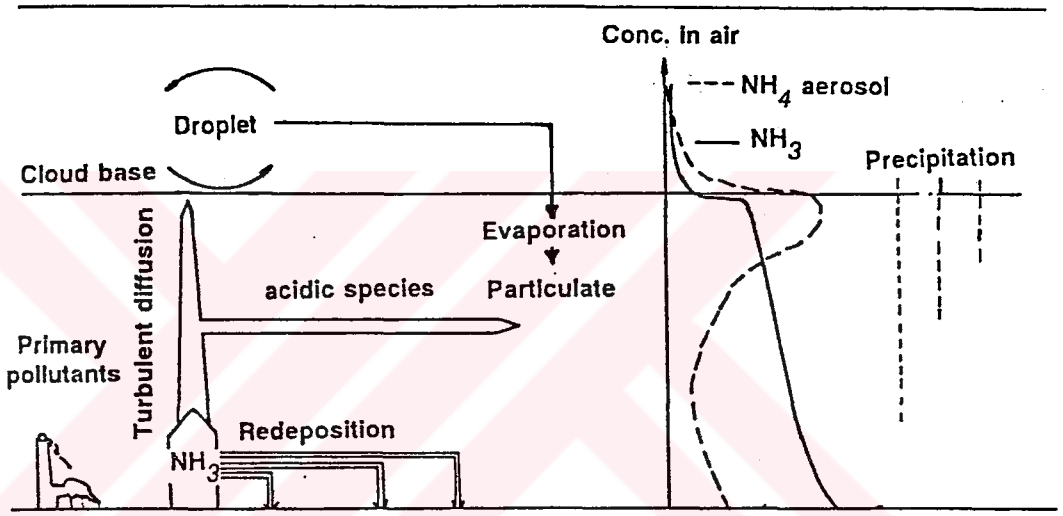

Figure 1.2 The fate of NH_3 emissions into the atmosphere

Figure 1.3. summarizes three ranges as well as the major sources and removal processes for each particles [1]. Particles with diameters ≥ 2.5 μm are usually identified as coarse particles and those with diameters <2.5 μm are called fine particles. The fine particle mode typically includes most of the total number of particles and a large fraction of the total aerosol mass, for example, about one-third of the mass in non-urban areas and about one-half in urban areas. The fine particle mode can be further broken down into particles with diameters between approximately 0.08 and 1-2 μm, known as the accumulation range and those with diameter ≤ 0.08 μm, known as the transient or Aitken nuclei range.

Particles in the coarse particle range are usually produced by mechanical processes such as grinding, wind or erosion. As a result, they are relatively large and settle out of the atmosphere by sedimentation except on windy days where fallout is balanced by reentrainment. The majority of biological particles, spores, pollens, sand and sea salt tend to be in the coarse particles.

Because of the nature of their source, particles in the accumulation range generally contain for more organics than the coarse particles (other than biologic particles), as well as soluble inorganics such as NH_4^+, NO_3^-, SO_4^{2-} and so on.

Particles in the accumulation range tend to represent only a small portion of the total particle number (e.g. 5 %) but a significant portion (e.g. 50 %) of the aerosol mass. They have large surface area and many trace elements from combustion processes attach on these aerosols. Because they are too small to settle out rapidly, it is important to sample them in

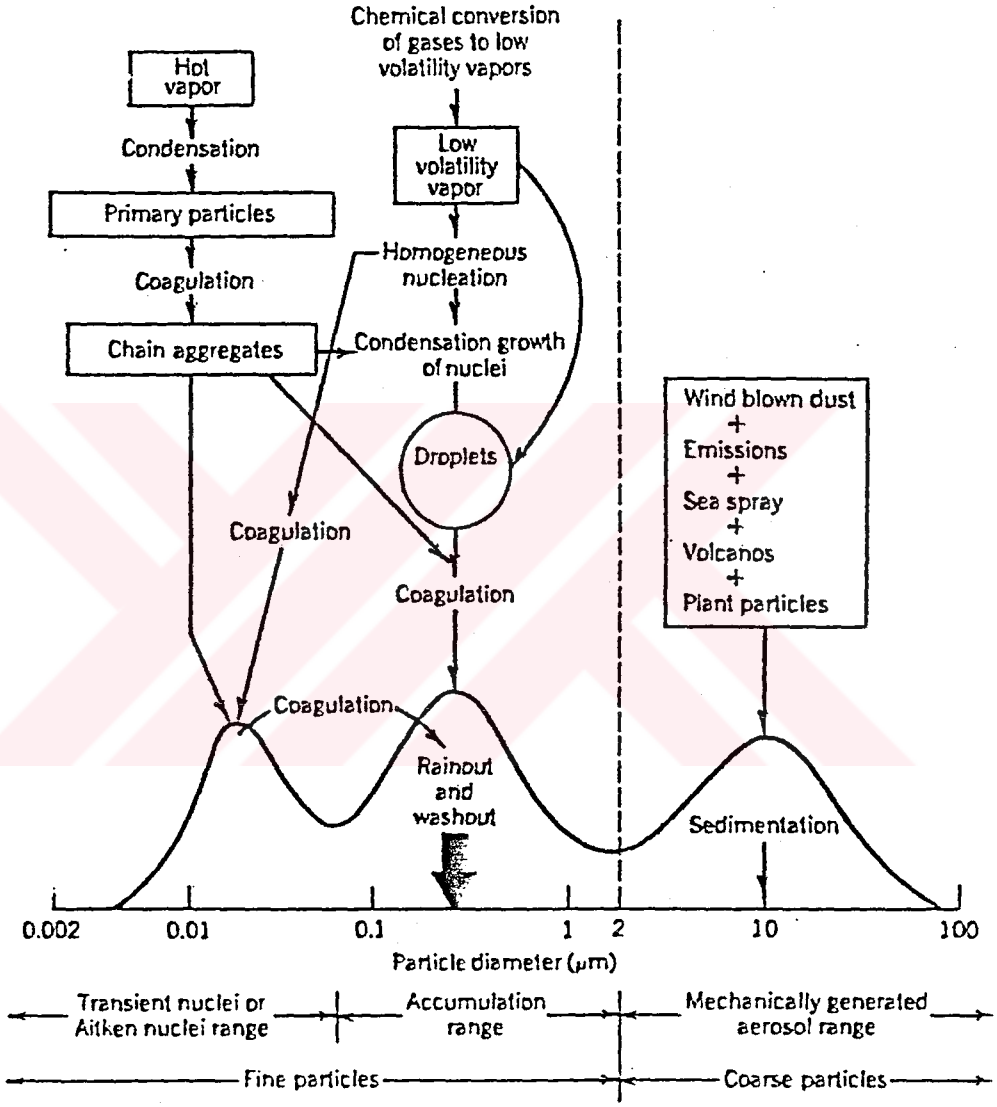

Figure 1.3 Schematic of an atmospheric aerosol size distribution showing the three modes, the main source of mass for each mode

order to follow the pollution sources by using PM-10 inlet. They are removed relatively slowly by incorporation into cloud droplets followed by rainout or by washout during precipitation. They may be carried out to surfaces by eddy diffusion and advection and undergo dry deposition. As a result, they have much longer lifetimes than coarse particles.

Aitken nuclei arise from ambient temperature gas-to-particle conversion and combustion processes in which hot, supersaturated vapors are formed and subsequently undergo condensation. These particles act as nuclei for the condensation of low-vapor-pressure gaseous species causing them to grow toward the accumulation range and so these nuclei may grow larger by coagulation. This range contains most of the total number of particles but relatively little of the total mass because of their small size. The lifetime of these particles is short, sometimes on the order of minutes, due to rapid coagulation.

Fine particles in the 0.1-2.0 μm size range are effective at scattering light and soot (lower 0.1 μm) is also effective at absorbing light in the shortwave range close to the ground. These effects contribute to a reduction in visibility through the atmosphere and they affect intensity of solar radiation reaching to the surface, and terrestrial radiation escaping to the space. They also can affect the human respiratory system. In a clean air the visibility distance can be over 50 km but in air polluted by particles this can be severely reduced. A mass concentration of 200-300 $\mu g\ m^{-3}$ will reduce the visibility to below 5 km. Additionally, ions and radioactive products may attach to the particles, so they control electrical and radioactive properties of the atmosphere. Deposition of atmospheric

particles can be an important source of marine pollution as well as soil pollution.

1.2.3. Droplets

Droplet means a small liquid particle of such size and density as to fall under still conditions, but which may remain suspended under turbulent conditions [4]. Very small particles in the Aitken range act as condensation nuclei for the formation of larger particles in a supersaturated vapor. If these very small particles are injected into air which is supersaturated with water or another vapor such as an alcohol, the vapor condenses on them to form droplets [2].

The gas phase oxidation of primary pollutants to secondary pollutants is important. However most reactions occur in the atmospheric droplets. These reactions play an important roles in problems such as acid rain, fogs and in the growth and properties of aerosols. The aqueous phase which serves as a reaction medium in the atmosphere is present in the form of clouds, fogs, rain and snow also, particulate matter consisting of an aqueous solution containing pollutants may provide the liquid phase for reactions; thus at typical relative humidities, approximately 30-50 % of the aerosol mass is due to water [2].

If gas phase reactions are the only ones in the oxidation of SO_2 to SO_4^{2-}, conversion should be very low during the winter months. Although SO_2 to SO_4^{2-} conversion decreases a little during winter, because both the solar intensity and the length of day are reduced and the effect of reduced solar intensity may also be expected to continue into aqueous

phase processes since the winter time concentrations of photochemically produced soluble oxidants(e.g. H_2O_2) should be lower than in summertime however, it never approaches to zero in droplets [6].

Water droplets can accumulate pollutants by adsorption of either gases or particles, and within the droplets chemical reactions can proceed, changing the nature of the adsorbed species. In cloud processes, the most important oxidants appear to be ozone and hydrogen peroxide, both of which first are adsorbed by water from the gas phase [7].

Gas O_3 SO_2

$\downarrow$ $\downarrow$

Solution $O_3 + SO_2 + H_2O \rightarrow 2\,H^+ + SO_4^{2-} + O_2$

Sulfuric acid formed will be completely dissociated into H^+ ions and SO_4^{2-}. Usually, aqueous phase oxidation of SO_2 is catalysed by metal ions (Fe^{3+} or Mn^{2+}) or soot. Although there may be partial neutralization by ammonia, water in polluted fogs and clouds can be much more acidic than rain and snow. Since evaporation of the fog droplets can result in very high concentrations of ions in a strongly acidic liquid phase and because of their smaller diameters, fog droplets have larger surface area therefore higher concentration pollutants. Such acid fogs are major health concern because the droplets are sufficiently small to be inhaled as they are located closer to the ground. Indeed, fogs with pH values < 2 have been observed in heavily populated coastal cities in Southern California.

Both photochemical reaction and aqueous phase oxidation of SO_2 leading to H_2SO_4 are important. However for nitrogen oxides, dominant

process is the gas phase oxidation to HNO_3 followed by absorption into water. This arises because of the poor solubility of NO_2 and especially NO in water.

1.3. Deposition Phenomena

Atmospheric deposition is a term that refers to solid, liquid, and gaseous materials deposited by atmospheric processes [8]. Both natural and anthropogenic constituents reach the surface of the earth through two pathways: 1) wet deposition 2) dry deposition. Rain and snow comprise wet deposition, whereas settleable particulates, aerosols, and gases comprise dry deposition. Depending upon the chemical composition of the pollutants, they can have a variety of impacts on the aquatic and terrestrial ecosystems in which they deposit [9]. Depositions are final steps in removal of atmospheric constituents. The efficiency of wet deposition is controlled exclusively by atmospheric processes (precipitation physics and chemistry), whereas the rate of dry deposition is mainly controlled by the surface onto which the constituents are deposited [10].

1.3.1. Wet Deposition

The phrase wet deposition encompasses all of the processes whereby pollutants attach to atmospheric water in the form of rain or snow or fog [11]. Wet deposition may become relatively more important than dry deposition, depending upon the pollutant. Aerosol particles allowing growth of droplets are called cloud condensation nuclei [12]. The stage of cloud condensation is followed by glaciation and eventually, precipitation. In the majority of cases, however, clouds reevaporate without precipitation.

In-cloud absorption followed by precipitation is termed "rain out; below-cloud absorption, i.e. pollutants collected as the drops fall, is termed "washout". The rate of removal of a pollutant by wash-out will increase in proportion to the precipitation rate. In remote areas the majority of the wet deposition of pollutants appears to be due to rain-out. Wash-out becomes relatively more significant near the sources of pollution.

The wet deposition process is a major pathway of acidic pollutants from the atmosphere to the biosphere. They involves complex chemical transformation of SO_2 and NO_2 to H_2SO_4 and HNO_3 in a cloud as well as the processes of cloud formation, precipitation, the interaction of fog droplets with the Earth' s surface [13].

1.3.2. Dry Deposition

Pollutants in the form of either gases or small particles can be transported to the ground level and absorbed and/or adsorbed by materials there without first being dissolved in atmospheric water droplets; this is called "dry deposition" [1]. It should be noted that the surface itself may be wet or dry; the term dry deposition only refers to the mechanism of transport to the surface, not to the nature of the surface itself. Dry deposition involves sedimentation and impaction as well as turbulent and molecular diffusion. Except for large aerosols, whose sedimentation velocities exceed turbulent velocities, dry deposition is determined by surface properties such as roughness, adhesiveness, stability and wetness [9].

1.3.3. Effect of Wet and Dry Deposition to Forest Ecosystem

Acid deposition and its effects were recognized at a local scale as early as the middle of the 17^{th} century. The problem was well defined and documented in Great Britain and parts of Europe nearly two centuries later by Robert Angus Smith during the period between 1852 and 1872. The deleterious effects of industrial emissions on plants, animals humans and the atmospheric transport of pollutants between England and France had become issues of concern. It is interesting that over three hundred years ago in England, recommendations were made to move industry outside of towns and build higher chimneys to spread the pollution into distant parts. It then rapidly sank from visibility in both scientific and public sectors. However it became an actual topic again a century later having grown in the intervening time period from a locale scale problem to one of global proportions [8]. Acid deposition affects both aquatic and terrestrial systems in nature as well as it has other effects on the environment and humans. we will concern on the effect of acid deposition on forest ecosystems. The much greater efficiency with which wind-blown cloud is captured by vegetation with large aerodynamic roughness. Calculations and direct measurements of cloud droplet capture have shown that deposition rates to forest may be four times that to grass, and that cloud water can contribute over half the wet deposition of solutes to upland forests.

In parts of North America, Europe, and Scandinavia, forest damage, caused directly or indirectly by acid deposition, has been observed in various species of trees. In Czechoslovakia, much of the forest in the Erzgebirge region has died and the remainder shows severe damage. In Germany, the Black Forest and forests in parts of Bavaria have undergone

extensive dieback. In North America, forest damage appears to be confined largely to high elevation red spruce forests in the eastern and northeastern parts of the continent [8]. Forest declines may have important effects extending beyond wood production. Forests fulfil essential functions (e.g. the maintenance of genetic diversity, the provision of wildlife habitats, landscape protection and recreation). They also play an important role in the hydrological cycle [14].

It is impossible to obtain separate measurements as both deposition forms are associated with processes which occur in the forest canopy. The dry deposition is most important close to major air pollution sources and is usually responsible for any direct damage to plant. However, dry deposition may also be important in remote areas and it should not be ignored [11].

Although natural processes affect the chemical composition of atmospheric deposition, anthropogenic pollutants are overwhelmingly important. Especially sulfur and nitrogen compounds may be transported tens to hundreds of kilometers from their source by air masses before they finally return to the earth as acid deposition. During transportation, they are oxidized and combine with water vapor to form sulfuric and nitric acids, sulfate aerosols and particulate sulfate. Much of the NO_x is emitted closer to its source. The chemical constituents of precipitation deposition in remote areas are mainly hydrogen, sulfate, nitrate and ammonium ions, but other substances such as trace elements or organics scavenged from the atmosphere may be present. High-altitude forest sites receive a higher loading, despite their distant location from major emission sources, because

of orographic effects, high wind speeds, cloud immersion and the open nature of the large surface areas, particularly of spruce canopies [14].

Although a direct causal link between forest damage and acid deposition has not been made, enough damage by acid deposition may occur which weaken the tree and enhance its susceptibility to factors such as cold climate shocks, insect attacks and other pollutants such as ozone and SO_2. The combinations of NO_2 with SO_2 and O_3 have proven to create even more drastic effects. Since the influence of such a combination can further stimulate the leaching of various elements from foliage. the dose of aqueous pollutants depends on concentration and contact time and both factors are strongly dependent on weather condition. For a given rain or cloud event, the volume of liquid in contact with a leaf depends on deposition rate and leaf wettability and water holding capacity, which in turn depends on wind speed and mechanical disturbance.

Sulfuric acid and HNO_3 affect leaf tissue directly, if pH is low enough to overcome the buffering capacity of the leaf. The indirect impact of air pollution on trees occurs as a result of changes to chemical and biotic properties of soils which affect the tree by altering the structure and functioning of the rooting system and by the loss of ions resulting in large-scale nutrient imbalances, frequently causing discoloration of needles and leaves. Sulfate and nitrate deposition has made soils more acidic, leaching basic cations and leading to the mobilization of aluminum which in some cases; has reached potentially toxic concentrations. Aluminum ions may damage root hairs and produce sites for pathogens to enter. Important microbiological processes such as mineralization is reduced by high soil levels of aluminum. Magnesium and calcium deficiency may cause dieback

at high elevations with acidic bedrock. Magnesium deficiency also reduces photosynthesis and growth, and reduces resistance to temperature stress. While nitrogen is a vital nutrient most plants have evolved methods to live with low levels. Saturation would spur growth, forming large cells which are easily attacked by wind, drought, and parasites. Strong acids also dissolve wax in leaves and disturb stomatal functions. Nitrogen taken up may also be changed to toxic ammonia, forcing plants to drop leaves to eliminate the toxin. Absence of Ca, Mg, and K causes a reduction in root respiration, eventually damage to fine feed roots and to root morphology.

Ammonium and nitrate ions contribute significantly to the pH of precipitation and form important soil nutrients via soil-water or foliage. However, there are indications that forests in some parts of Europe have reached saturation levels for nitrogen. Assuming this is true, the excessive wet and dry deposition of N compounds could be a possible cause of die-off in Europe [14].

1.4. Snow Chemistry

1.4.1. Scavenging Power of Snow

It is well known that clouds and precipitation contributes significantly to the removal of atmospheric pollution [15]. Formation of snow flakes is followed by the following path : Hydrometeors in clouds may begin as ice nuclei or condensation nuclei. In the former, an atmospheric particle in an air mass saturated with water vapor serves as the nucleus of a snow or ice crystal which grows by water vapor diffusion or accretion cloud droplets. The droplets may be supercooled, existing in a liquid state far below freezing. Temperatures must be -5 ^{o}C or lower to activate particles as ice nuclei; colder temperatures result in a faster rate of crystal growth, reaching a maximum rate at about -15 ^{o}C. Decreased atmospheric pressure also increases the growth rate. Clay mineral particles derived from the earth's crust make good ice nuclei [16].

The gas phase scavenging is important especially for nitrate. The nitrate in snow comes primarily from the scavenging of particulate nitrate and HNO_3, although the scavenging of other nitrogenous compounds such as HNO_2, PAN (peroxyacetyl nitrate) or NO_2 could contribute. The sulfate present in snow may be due to the both particulate sulfate and SO_2 [17,18].

For some species, scavenging power of winter rain and snow may be different. For example scavenging of NO_3^- ion with the winter snow is much more efficient than the winter rain. It is suggested that since both winter rain and snow originate from sub-freezing clouds, the higher NO_3^-

concentrations found in snow than in rain must be due to more efficient below cloud scavenging of N species in the air by snow flakes than rain drops and also the snowflakes scavenge gas phase HNO_3 more efficiently than raindrops because of high adsorption of HNO_3 in snow [19]. This may be due to the precipitation depth which is at least 4 times more for rain than for snow events [17,18,20] and high scavenging of snow for aerosol may be related to the increased contact area of snow with respect to rain [19]. In other study, the higher concentrations of H^+, SO_4^{2-} and NH_4^+ were found in winter rain compared to snow [21].

How airborne contaminants become incorporated into snow ? There are several processes by which this incorporation can occur:

(a) Airborne particles may serve as cloud condensation nuclei or ice nuclei during formation of hydrometeors.

(b) Cloud droplets or ice crystals may scavenge particles and gases as air sweep through clouds.

(c) Airborne particles and gases below the cloud base may be scavenged by falling snow [16].

In-cloud scavenging is usually the dominant removal mechanism for accumulation mode particles (0.1-1 μm) [22]. Depending on the elevation of a measuring site, below-cloud scavenging may add a significant contribution to the overall scavenging. Below-cloud scavenging of aerosols are more efficient for larger particles. For crustal components there is a good correlation between atmospheric concentrations from ground level measurements and deposition concentration.

The theoretical investigation of the removal of high altitude aerosol from the atmosphere is undertaken by considering the aerosol motion to be determined by a super position of forces. An initial assumption is made that the ice crystal falls in a steady state offering maximum resistance to the direction of the motion. Scavenging of atmospheric species are possible by one of the following mechanisms [23].

Impaction: Because of the relative settling rates of the water drop and the particle in a gravitational field, collision between the two becomes possible. Aerosols leave the flow of air around the crystal because of their momentum and then impact on the crystal. This becomes the dominant mechanism for aerosol > 7-8 μm in size.

Interception: The mass centers of the aerosol particles would follow the flow of air around the crystal but their physical size causes capture. This is the dominant mechanism of capture for aerosols in the size range 0.5 μm < diameter< 8 μm.

Brownian deposition: This is just the collection due to the Brownian motion of the aerosol. Brownian motion as the term applied to the irregular motion of particles in response to their thermal bombardment by gas molecules. If the water drop is stationary with respect to the air, the Brownian motion of the particles alone will give rise to collisions. This process is termed Brownian diffusion. This becomes modified by the flow of air around the collector and is the main collection mechanism for particles < 0.5 μm.

Electrostatic effects: If the water drop and the aerosol particle are charged, there may be a significant modification to the capture rate. Similar charges will tend to inhibit collisions, while dissimilar charges will tend to encourage them. However it is not necessary for both the drop and particle to carry a net charge. Electrical effects may still occur even if only one is charged

or if they are uncharged but polarized by an existing electric field within or below the cloud [24].

Phoretic effects: These are enhancements of the collection efficiency due to gradients of temperature and vapour pressure around the collector. The magnitude of the effects are complex functions of the respective fields. The effects have been shown to alter the collection of particles smaller than 1 μm.

Scavenging of species in the atmosphere are described by using the scavenging ratios. The scavenging ratio is defined as a dimensionless quantity [16].

$$W = \frac{C_s}{C_a} * d_a$$

Where W= scavenging ratio, C_s= concentration of contaminant in snow (μg/g), C_a= concentration of contaminant in air ($\mu g/m^3$) and d_a= density of air (g/m^3).

Determination of W requires simultaneous measurement of concentrations in snow and in surrounding air. Most scavenging ratios have been calculated using ground-level measurements of atmospheric concentrations measured over a period of time longer than that of the precipitation event. Therefore, the assumption has to be made that the atmospheric concentrations of the measured species are vertically and temporarily constant during the measurement period, which is essentially not correct. This concept also assumes that total deposition is dominated

by wet deposition and contribution by dry deposition is negligible [16,22]. A large number of factors can affect the scavenging ratios such as snow crystal type and size, aerosol particle size, precipitation depth, riming, vertical concentration gradients, cloud height, air temperature, relative humidity and electrical charge [17,22].

1.5. Research Done on Chemistry of Snow and Aerosol in Rural Areas

L. Clint Duncan and his group analyzed the composition of precipitation in the central cascades of Washington State. Bulk precipitation samples were collected weekly during the winters of 1984 and 1985 at two high elevation sites. The cascade sites are downwind and are within 60 km of significant acidic oxide point and other sources. The precipitation was found to be low in contaminant content with SO_4^{2-}(9.88 μeq/L) and NO_3^- (10.27 μeq/L) concentrations as low or lower than those reported for remote stations in the US or elsewhere [25].

Duncan did another research on snow composition in the Washington Cascades in 1989. His research constituted rime composition also. Sampling method was same and it was found that snow composition did not differ from the previous one. However the rime samples on the average were 1.8-4.5 times more concentrated than cocollected snow in nitrate, sulfate and ammonium ion [26].

Composition of snow in pacific coastal mountain in Canada were investigated. A snow collection sites were all in mountainous regions at altitudes from 945 to 2069 m above sea level. Three types of samples were collected. Profile samples were obtained by digging into snowpack to a

depth of about 3 m. One-metre core samples were obtained using semi-cylindrical plastic coring device. Surface samples were taken of the top 20 cm of snow in the surrounding 100 m diameter area. Because of the relatively low concentrations of chemicals in the snow, Many of the concentrations were below the detection limit. They reported average values of three sites in μeq/L: [SO_4^{2-}]< the detection limit; [NO_3^-] = 2.4 ; [NH_4^+] = 1.1 ; [Ca^{2+}] = 2.2 and [H^+] = 4.2. The average pH was 5.4. Statistical analyses indicated that most of Na, Cl and Mg ions were of sea water origin. Ammonium ion was highly correlated with nitrate ion. This suggested that NH_4NO_3 was an important salt in the precipitation. In the Vancouver area, the concentrations were higher and variable. The increase in sulfate values, compared to previous sites, was attributed to the anthropogenic sources around Puget Sound and Goergia Strait. Sulfate was found to provide about one-half of the acidity and that nitrate and carbonate about one-quarter [27].

Heavily-contaminated (black) snowfalls frequently occur in Cairngorm Mountains (Scotland) in spite of their relative remoteness from major source regions. Daily samples of snow were collected at 1100 m and the reported results from the analyses of major ions and trace metals. The heavily-contaminated snowfalls were associated with back-trajectories which originate in the east (Eastern Europe, European U.S.S.R. and the Baltic). Correlation and factor analyses of major ions, trace elements and particulate concentration data indicated that components from crustal and anthropogenic sources behave quite similarly. It was not possible to apportion by source on the sub-regional sources. There was no evidence of contaminant concentration enhancement with increasing altitude in terms of long-term (weeks-months) mean snowfall composition [28].

Aerosol measurements were made from a remote continental site Mallikadevi (India), 1500 km from the nearest coast and 2200 m above sea level in the midst of a pine forest. The sampling period was 6-8 h during day and 12 h during the night. Precipitation samples (26) were collected on a 24 h basis. Of the 18 elements measured, the concentration levels of Pb, K, Zn and Br showed marginal enrichments relative to their crustal abundances using Fe as the reference element. Factor analysis indicated specific source patterns more closely related to biomass combustion and a complex mixture of components derived from natural and 66 pollution sources. The observed SO_4^{2-}/ Na^+ ratio of 0.55 showed sulfate excess as compared with sea salt ratio of 0.25 possibly again from combustion of biomass and fuel wood in the local environment in the wet deposition. The wet deposition chemistry indicated the importance of calcareous soil derived materials and sea salt elements with marginal enrichment for Zn, Sb, S, K and Br. Because of the very low concentration levels comparable with data reported from other rural sites, Mallikadevi can be considered as a background site from the Indian subcontinent [29].

Powassan which contains no significant industry is a rural location in Southern Ontario. Pollution sources are mainly domestic heating and automotive. Continuous measurements of concentrations of trace gas and aerosol species were done from 20 January to 24 February 1984. The sampling site was free from local sources of pollution. The measurements included aerosol H^+, NH_4^+, Na^+, Ca^{2+}, NO_3^-, SO_4^{2-} and Cl^-, gaseous SO_2, NO, NO_y(= NO+NO_2+PAN+HNO_3+ aerosol NO_3^-), HNO_3, PAN and O_3. The measurements showed that concentrations of both primary and secondary pollutants were quite high during winter. Clear air t-NO_3^-(aerosol NO_3^- + HNO_3)/SO_4^{2-} ratios averaged 5-10 times higher in winter than in

summer which suggested that HNO_3 was a more important source of atmospheric acidity, relative to SO_4^{2-} aerosol. Factor analysis showed that high factor loadings between HNO_3, SO_4^{2-} and aerosol H^+. The concentrations of most pollutants were highest when trajectories were from north with the location of NH_3 sources. The SO_2 and SO_4^{2-} concentrations were not highly correlated ($r^2 = 0.18$). Sulfates exhibited a much stronger correlation with t-NO_3 ($r^2 = 0.58$) and NO_y ($r^2 = 0.58$). Observations suggested that concentrations at Powassan were characteristic of broad regions of northeastern North America in winter [6].

Daily samples of atmospheric aerosol have been constantly taken in Preila which represents the rural site of Lithuania since 1980. Concentration of major cations and anions have been determined. A seasonal variation is typical of the major aerosol components. The alteration of daily concentrations of chemical components was discussed in conjunction with meteorological conditions. Air masses from western Europe have been concluded to bring the greatest amount of anthropogenic pollutants to Lithuania [30].

Aerosol samples were collected at four high elevation sites (>5000 m) in the mountains of central Asia. Daily samples were collected over periods of four days to two weeks in late summer. This period is typically one of relatively low levels of dust in the Asian troposphere. Aerosols were dominated (in order of importance) by NH_4^+, SO_4^{2-}, NO_3^- and Ca^{2+}. Concentrations of these species were comparable to previously reported measurements in the remote troposphere. Aerosol showed very high levels of Ca^{2+}, SO_4^{2-}, Cl^- and Mg^{2+} due to the influx of evaporite mineral rich dust derived from the Qaidam Basin and Taklamakan Desert. High-elevation

mountain sites in the Himalayas and Southern/central regions of the Tibetan Plateau provide isolated platforms above the planetary boundary layer from which to investigate the composition of the remote continental troposphere. Fresh and surface snow samples were also collected. The results showed that the general composition and spatial pattern in summer snow chemistry was similar to that for aerosols [31].

1.6. The Aim of This Study

A monitoring station which is equipped with automatic analyzer for the gas phase pollutants (SO_2, NO_x, O_3) and total suspended particulates (TSP) and meteorological parameters (wind speed and direction, temperature and humidity) has been in operation since March 1993. The area is suffering from severe pollution damage. Lack of aerosol and wet deposition data in this sampling site urged us to consider the collection of aerosol and snow samples. Snow constitutes the large portion of the precipitation in Uludağ. Because of its unique scavenging or cleaning properties, precipitation is known as a useful indicator of ambient pollution level concerning with the inputs of harmful compounds to terrestrial and aquatic biota. In addition to this, aerosols are known to play a vital role in acidification of clouds, precipitation and fogs.

The aim of this study to determine chemical composition of aerosol and snow in Uludağ in relation to contributing sources and local meteorology. Observed trends in chemical compositions are discussed considering interrelation of three different phases namely, aerosol, gaseous and liquid phases.

CHAPTER II

EXPERIMENTAL

2.1. Sampling Site

The sampling site, Sarıalan region of Uludağ Mountain which has an 1685 m altitude and located at about 10 km south of Bursa which is the fifth largest city in Turkey with the population around three million. Bursa is one of the polluted city of the country due to large industrialization, domestic coal burning and its geographical location. The selected area is below the boundary layer and thus it is possible to sample the polluted air below inversion layer. This place is chosen considering some important points like height of the sampling site, local meteorology, distance to local pollutant sources and to the trees which are 100 m away from the station. It was not feasible to go very far away from the roadway and electricity because of the severe winter conditions. Motor vehicle emissions are also important source of pollution, especially during summer months since the city is located on the highways connecting eastern and southern cities to Istanbul. This region is about 7 km away from hotels in the ski resort area at the south to south-east direction which may be the potential source of the pollutants. It is also expected that some of the pollutants come from European Countries with

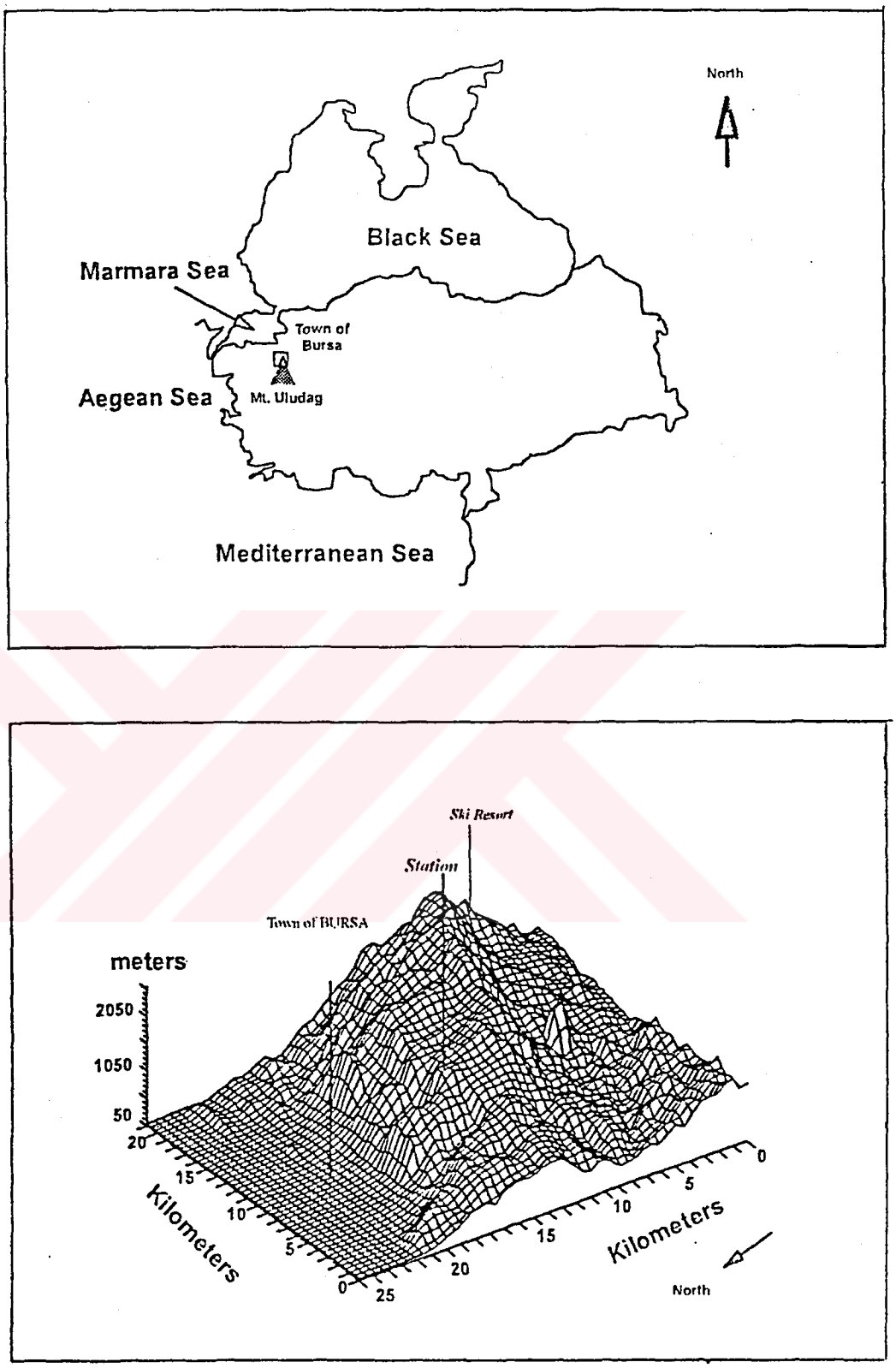

Figure 2.1 Location and topographical feature of the sampling site

the north winds. Apart from these, marine aerosols could be another source because Marmara Sea is 30 km north-west of Uludağ Mountain and Aegean Sea is 200 km west of it. Another potential source of the pollutants is Orhaneli coal fired power plant lying at 30 km south to south west of the station.

2.2. Sample Collection and Handling

Collected snow and aerosol samples in Uludağ Mt. were brought in Ankara with using polyethylene containers in order to minimize adsorption and desorption of species to and from the containers during sampling, storage and analysis. All containers and funnel were rinsed several times with double distilled deionized water in order to minimize contamination. Polyethylene gloves were used during the collection of samples and preparing them for analysis. Another potential source of contamination is the air of the laboratory in which samples are prepared for the analysis. Therefore, samples were handled under HEPA (High Efficiency Particulate Filters) filters made up of a combination of cellulose and mineral fibers in a class-100 clean room in Environmental Engineering Department in METU. There are four HEPA which remove particles greater than 0.1 μm with 99.997 % efficiency. One of them pulls air from outside the room and after filtering send it inside. Other three filters refilter the filtered air in the room [32].

All chemicals used were analytical grade and superpure nitric acid from Merck. All solutions were prepared with double-distilled deionized water obtained from Nanopore, Ultrapure Water Purification System. Polyethylene material used for AAS analysis was cleaned by soaking in

10 % (v/v) nitric acid solution for at least one day prior to their use. To the samples allocated for the AAS analysis two or three drops of superpure nitric acid were added in order to leach the cations from the surface of the bottles.

2.2.1. Aerosol Sampling and Sample Preparation

Aerosol sampling was done daily during the period September 1993 - April 1994 with TSP analyzer installed in a rack in the station. The aerosol samples are collected on a glass fiber filter at high air flow rate (25 L/min) as a 1 cm diameter spots. Glass-fiber filter paper is chosen because it does not cause pressure drop. The size of the particles that has been measured by this analyzer is less than 10 μm. After sampling the filter paper was kept in the polyethylene bags. Under the HEPA filters each spot on the continuous filter paper was cut and transferred to the closed petri dishes until analysis. Filter blanks were treated with the same way. During the analysis, aerosols were extracted with 10 mL deionized water by using ultrasonic shaker (Branson Model 2200) for 15 min and filtered through a 0.2 μm size nucleopore filter paper. The aqueous extract analyzed for water soluble cations and anions. Approximately 2-3 mL of this extract was used for Ion chromatography. One mL of the solution diluted to 10 mL with reagents and water and was used for ammonium determination colorimetrically with Nesslerization method. Remaining extract (5 mL) was diluted to 10 mL was analyzed by flame Atomic Absorption Spectrometry (AAS) and Atomic Emission Spectrometry (AES) for the major cations.

2.2.2. Snow Sampling and Sample Preparation

Snow sampling was done weekly because of hard winter conditions during the period December 1993 - April 1994. The snow collector was designed in our laboratory as shown in Figure 2.2. It is consisted of silk asbestos, resistances, a thermostat positioned 2-2.5 m above the snow surface. Resistances were placed in the silk asbestos and this cover with a thermostat (15-30 ^{o}C) was circulated on the outer walls of the polyethylene funnel to melt the snowflakes. Snow flakes was melted as soon as it fell in the funnel and snow water was collected in a barrel inside the container, by this way contamination of samples were avoided.

Samples of double distilled deionized water were carried into the field and analyzed as field blanks. Prior to analysis, after pH measurements and filtration using 0.2 μm size nucleopore filters. The snow samples were divided into three fractions and stored in the freezer at -4 ^{o}C. One of the fraction was used for the determination of Ca^{2+}, Mg^{2+}, Na^{+} and K^{+} by flame AAS and AES and the second fraction was used for the determination of Cl^{-}, NO_3^{-} and SO_4^{2-} by Ion Chromatography and the last fraction was allocated for the determination of NH_4^{+} colorimetrically.

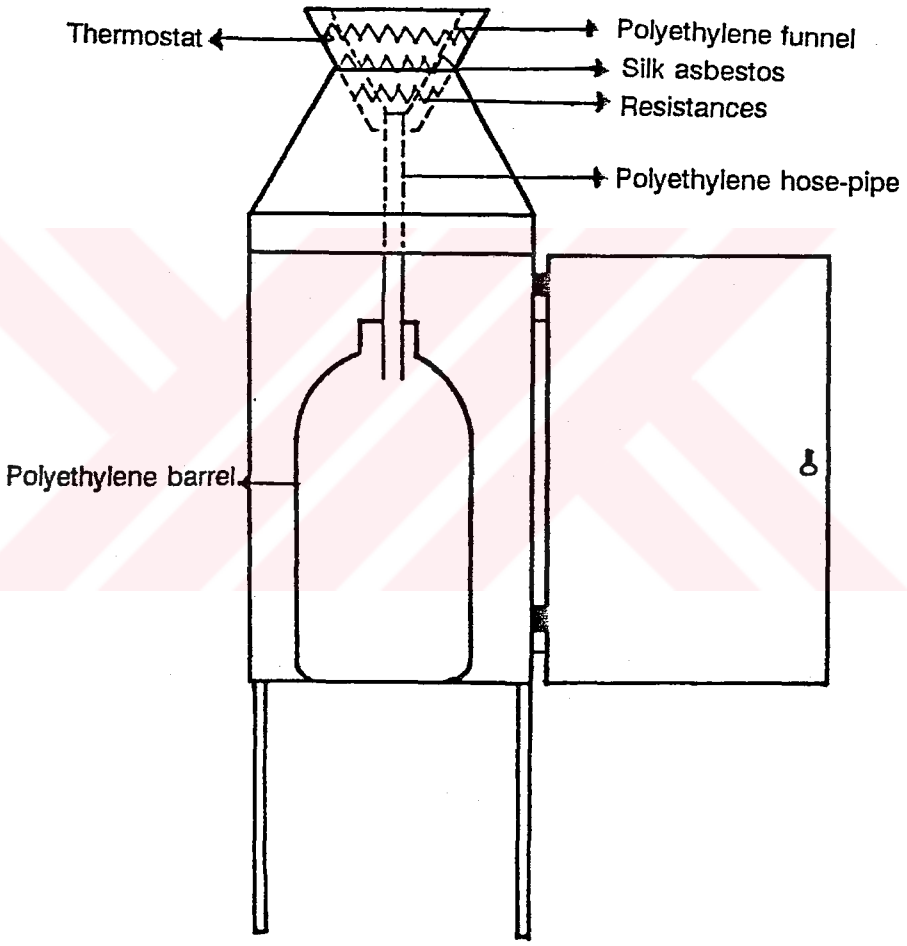

Figure 2.2. A schematic representation of the snow sampler

2.3. *Analytical Techniques*

Analytical methods used in this work are summarized in the Table 2.1

Table 2.1 Ions and analytical methods.

IONS	METHODS	INSTRUMENT
H^+	Electrode	Cole-Parmer Instruments Co. 5985-8 model pH meter 60648 model electrode
SO_4^{2-}	IC	Varian Corp. 302 IC Anion Column and Jasco 875 UV Detector
NO_3^-	IC	Varian Corp. 302 IC Anion Column and Jasco 875 UV Detector
Cl^-	IC	Varian Corp. 302 IC Anion Column and Jasco 875 UV Detector
Na^+	AES	Perkin Elmer model 1100 B Spectrometer
K^+	AES	Perkin Elmer model 1100 B Spectrometer
Ca^{2+}	AES	Perkin Elmer model 1100 B Spectrometer
Mg^{2+}	AAS	Perkin Elmer model 1100 B Spectrometer
NH_4^+	Colorimeter	Unicam 8625 UV/VIS Spectrometer

IC: Ion Chromatography
AES: Flame Atomic Emission Spectrometry
AAS: Flame Atomic Absorption Spectrometry

2.3.1. *Ion Chromatography*

Ion chromatography (IC) is a powerful tool for the determination of anions in environmental samples such as rain, snow, aerosol, fog and sewage owing to its advantage of fast, sensitive and accurate determinations of several anions at ultra-trace levels in one run within 10 min [33]. Several detectors are used in IC such as UV or visible, refractive

index, electrochemical and conductivity. The column packing material is high purity spherical silica with 20 μm in size and low surface area. Silica-based ion exchange column is preferred because of its better efficiency and overall performance than polymer-based columns.

The instrument we used in this research was equipped with a Varian pumping system, a Vydac 302 ion exchange column, a Jasco 875 UV detector. The eluent used was phthalic acid which absorbs in UV range (254 nm). Therefore a decrease in the background concentration was observed during the elution of the individual anion. This method is called as indirect UV method. The instrument was interphased to a computer for peak fitting using a software Peak 2. During the analysis, the chromatogram was first observed on the screen of the computer then about ten minutes after the injection, three peaks of Cl^-, NO_3^-, SO_4^{2-} were obtained. Concentrations of the anions according to the calibration were calculated after the peak identification.

All solutions were prepared with double distilled deionized water and filtered with a 0.2 μm size filter paper to remove bacteria. Leaving the column in acetonitrile (30%(v/v)) also prevents the bacterial growth which shortens the column life when the column is not used for 2 days or more.

The sample was directly injected without pretreatment through a standard 100 μl loop and eluted by a mobile phase following through column at 3 mL/min. The eluent consisted of a mixture of phthalic acid (1mM) which is powerful eluent and sodium borate at a concentration such that the pH was close to 4.93-4.95. To prepare solutions; 0.3326 g phthalic acid was dissolved in sufficient amount of water and diluted to 2 L and

maximum amount of $Na_2B_4O_7$*10 H_2O was dissolved to give 1 L of solution. After preparation, the solutions were degassed by ultrasonic shaker for 15 min in order not to damage the exchange column. Solutions were prepared in room temperature.

Standard stock solutions for Ion Chromatography were prepared from NaCl, $NaNO_3$, K_2SO_4. One of the calibration curve data is given in the Table 2.2. The concentrations obtained for these anions agreed with the SRM (Standard Reference Materials)(NIST) simulated rain water 2694a-I and 2694a-II.

Table 2.2. A calibration data for anion analysis.

	Cl^-	NO_3^-	SO_4^{2-}
Slope	16.73	11.42	11.15
Correlation coeff.(r)	0.999	0.984	0.999

2.3.2 Flame Atomic Absorption and Emission Spectroscopy

A Perkin Elmer Model 1100B Atomic Absorption Spectrometer was used in absorption and emission measurements. For analyses air/acetylene (oxidizing flame) flame was used for the determination of the magnesium, calcium, sodium, potassium. Magnesium was determined by flame AAS; sodium, potassium and calcium were determined by flame AES.

Before starting the analysis, the instrument was allowed to warm for about 20 min. Alignment of the lamp, burner system and the flame were adjusted so that it could have given maximum sensitivity. Nebulization uptake rate was around 7-8 mL/min and an aspiration of the sample to the flame was given directly. Some working parameters are given in the Table 2.3. We calculated the SRM values by using both aqueous calibration curve and when it is necessary standard addition calibration curve. We chose the curve which gave the closest value with an error limit of 5-10 % of SRM which are SRM (NIST) 1646 Estuarine Sediment, SRM (NIST) 2704 Buffalo River and GSP-1 U.S. Geological Survey. Some of the aqueous calibration curve values used in calculations are given in the Table 2.4.

Table 2.3 Some working parameters in flame AAS and AES.

	Mg^{2+}	Ca^{2+}	Na^{+}	K^{+}
Wavelength (nm)	285.2	422.7	589	766.5
Slidwidth (nm)	0.7	0.7	0.2	0.7

Table 2.4 A calibration data for cation analysis in flame AAS and AES.

	Mg^{2+}	Ca^{2+}	Na^{+}	K^{+}
Correlation coeff. (r)	0.999	0.999	0.992	0.999
Slope	0.101	0.024	0.314	0.121

Standard stock solutions for flame analyses were prepared from $CaCO_3$ with minumum volume HCl to effect complete solution of the $CaCO_3$ (1000 ppm). 1000 ppm NaCl, KCl solutions and 1000 ppm magnesium solution prepared by using magnesium ribbon in a minimum volume HCl. In addition to these standard solutions, multielement solutions were also used for calibration.

2.3.3. Colorimetry

Ammonium ion was determined colorimetrically at 425 nm on a Unicam 8625 UV/VIS Spectrometer after having been complexed by Nessler's reagent to form yellow to brown color according to the below reaction [34]. The quartz cells used had an optical path length of 1 cm.

$$2\ HgI_4^{2-} + 2\ NH_3 \rightarrow NH_2Hg_2I_3 + NH_4^+ + 5\ I^-$$

For ammonium analysis standard stock solution was prepared from $(NH_4)_2SO_4$ dried at 100 ^oC for 1 hour.

2.3.4. pH meter

An aliquot of unfiltered sample of snow was taken for pH determination using Cole-Palmer Ins. Company 5985-80 model pH meter with 60648 model probe calibrated with pH 4.00 and 7.00 buffers.

2.3.5 Accuracy of Methods and Detection Limits of Ions in Aerosol

Accuracy and detection limits for aerosol samples are given in the Table 2.5. Accuracy of the methods was found by comparing the concentrations of ions in SRM obtained from our calibration curves with the certified concentrations given in the SRM tables for the measured ions. Concentrations of ions in SRM found by us were subtracted by certified values then divided by certified values and multiplied by 100. Detection limits were calculated by using the concentrations of filter blanks within 3 standard deviation. At least 10 replicate measurements were done for the filter blank solution for each ion. The standard deviation of all measurements was multiplied by three and this result was added to the average of ten measurements. Concentrations were given in $\mu g/m^3$.

Table 2.5 Analytical parameters for the measured ions in aerosols.

Ions	Detection limit ($\mu g/m^3$)	Accuracy (%)
SO_4^{2-}	0.14	4.5
NO_3^-	0.14	14
Cl^-	0.13	6.7
Na^+	0.39	10
K^+	0.004	3.5
Ca^{2+}	0.31	7.7
Mg^{2+}	0.019	0.30
NH_4^+	0.33	

CHAPTER III

RESULTS AND DISCUSSIONS

3.1. Ambient Concentrations of Measured Species and Comparison with Literature Values

Concentrations of major anions and cations of aerosol samples are presented in the Table 3.1. The statistical results include number of observations N, mean, geometric mean, standard deviation, median and range. All ions showed a log-normal distribution therefore, geometric mean represent all data set better than mean and also geometric mean and median values are close to each other. Sodium, calcium, magnesium, chloride and nitrate ions have high standard deviations and also their range are very large indicating that they have some spikes in their temporal variation whereas potassium, ammonium and sulfate ions show stable variations which can be inferred from their low standard deviations. In general, the highest concentrations correspond to the sulfate, SO_4^{2-}, and calcium, Ca^{2+}, with the values of 2.2 and 1.6 μgm^{-3}, respectively. This result can also be driven by looking at the Table 3.2 which shows the average levels of the aerosol constituents in different regions of the world and Turkey. Especially, the results of the average concentrations of the world wide remote areas confirm that the sulfate and calcium

Table 3.1 Summary of aerosol concentrations and meteorological data at Uludağ Mountain.

Variables	N	Units	Mean	G. Mean	Standard Deviation	Median	Range Min.	Range Max.
TSP	153	$\mu g/m^3$	27	16	43	14	3.3	379
K^+	178	$\mu g/m^3$	0.064	0.046	0.041	0.057	0.0010	0.23
Na^+	174	$\mu g/m^3$	0.67	0.35	1.2	0.40	0.0050	12
Ca^{2+}	145	$\mu g/m^3$	1.6	0.83	1.9	0.78	0.010	9.0
Mg^{2+}	180	$\mu g/m^3$	0.12	0.054	0.23	0.06	0.0010	2.5
NH_4^+	150	$\mu g/m^3$	1.0	0.67	0.83	0.81	0.022	4.3
Cl^-	158	$\mu g/m^3$	0.47	0.26	0.61	0.25	0.0030	3.8
NO_3^-	168	$\mu g/m^3$	1.0	0.61	1.2	0.67	0.011	8.8
SO_4^{2-}	172	$\mu g/m^3$	2.2	1.48	2.0	1.71	0.053	13
Temperature	158	^oC	1.5		6.8	0.61	-13	15
R. Humidity	158	%	70	66	20	74	25	99
W. speed	158	ms^{-1}	2.9	2.4	1.8	2.2	0.56	9.6

TSP: Total suspended particles, N: Number of observations.

Table 3.2 Average levels of aerosol constituents in different regions of the world and Turkey in $\mu g.m^{-3}$.

	World wide[35] (remote)	Belgium[35] (rural)	Black sea[36] Atmosphere Turkey	Antalya[37] Turkey (coastal)	Mallikadevi[29] India (rural mountaneous)	Ontario[6] Canada (rural continental)	This Work (rural mountaneous)
Cl^-	1.07	0.05	2.6±1.8	3.27±12.58	-	0.14±0.22	0.47±0.61
SO_4^{2-}	1.11	-	6.7±2.1	4.67±3.04	-	3.98±2.87	2.15±1.99
NO_3^-	-	-	2.6±0.8	1.25±1.02	-	1.16±2.21	1.00±1.21
NH_4^+	-	-	-	0.86±0.71	-	1.21±1.21	1.02±0.83
Na^+	0.87	0.14	2.6±2.0	-	0.13±0.06	0.15±0.19	0.67±1.18
K^+	0.12	0.18	0.2±0.07	-	0.11±0.06	0.04±0.12	0.06±0.04
Ca^{2+}	0.20	0.22	0.77±0.88	-	0.40±0.26	0.07±0.18	1.61±1.92
Mg^{2+}	0.17	-	0.34	-	0.19±0.10	-	0.12±0.23

concentrations are the highest ones. However, in overall, concentrations of the ions are not high and they are comparable with the concentrations of ions measured in the mountainous and rural areas. Comparing our data with the work done in Black Sea and Antalya atmosphere reveals higher concentrations of Na^+, Cl^-, Mg^{2+} and SO_4^{2-}. It is reasonable to have such high concentrations of Na^+, Cl^-, Mg^{2+} and SO_4^{2-} ions coming from the Black Sea and Mediterranean Sea. Other ions are in comparable range with our work. Average TSP value is very similar to the average TSP value of the Mahedevan's work done in Mallikadevi (India) with a value of 22 $\mu g\ m^{-3}$. Measured meteorological parameters such as temperature, relative humidity, wind speed, wind direction will be treated statistically to identify the pollution contributing sources in the next sections.

3.2. Temporal Variability

3.2.1. Time Series Variations of The Ions

Time sequence plots, as presented in Figure 3.1 and Figure 3.2, give an idea about the general behaviour of the data set and qualitative understanding about the possible origins. In the figures, scale that shows the months is not linear, because we did not have aerosol samples in some days of months. If ions behave in the same manner, they are correlated and may originate from same sources, when they are measured at a receptor site. Daily concentration variations are used to detect spikes which could be result of a different source or a sudden change in meteorological conditions. They are also used to calculate the background concentrations.

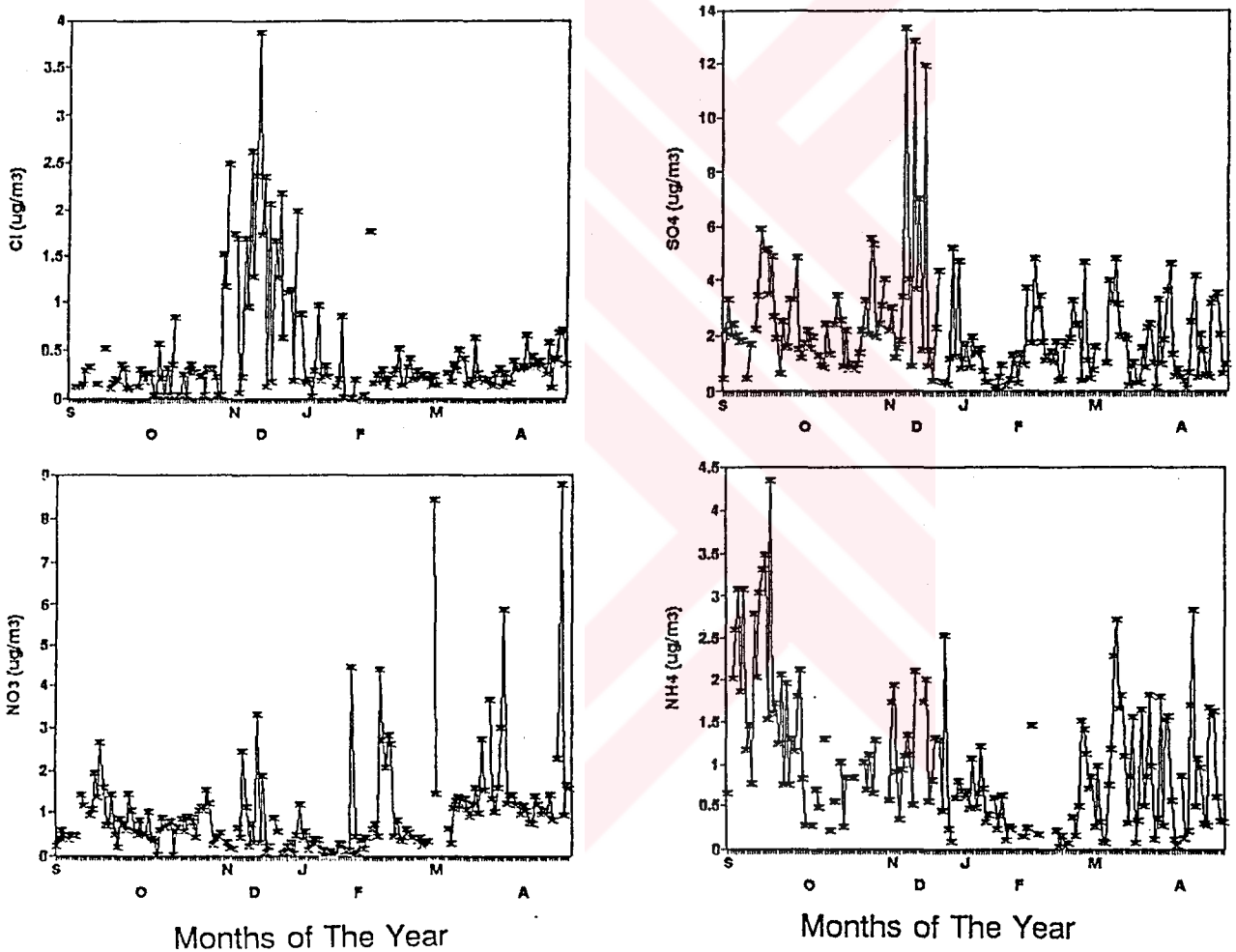

Figure 3.1 Time sequence plots of Cl^-, NO_3^-, SO_4^{2-} and NH_4^+

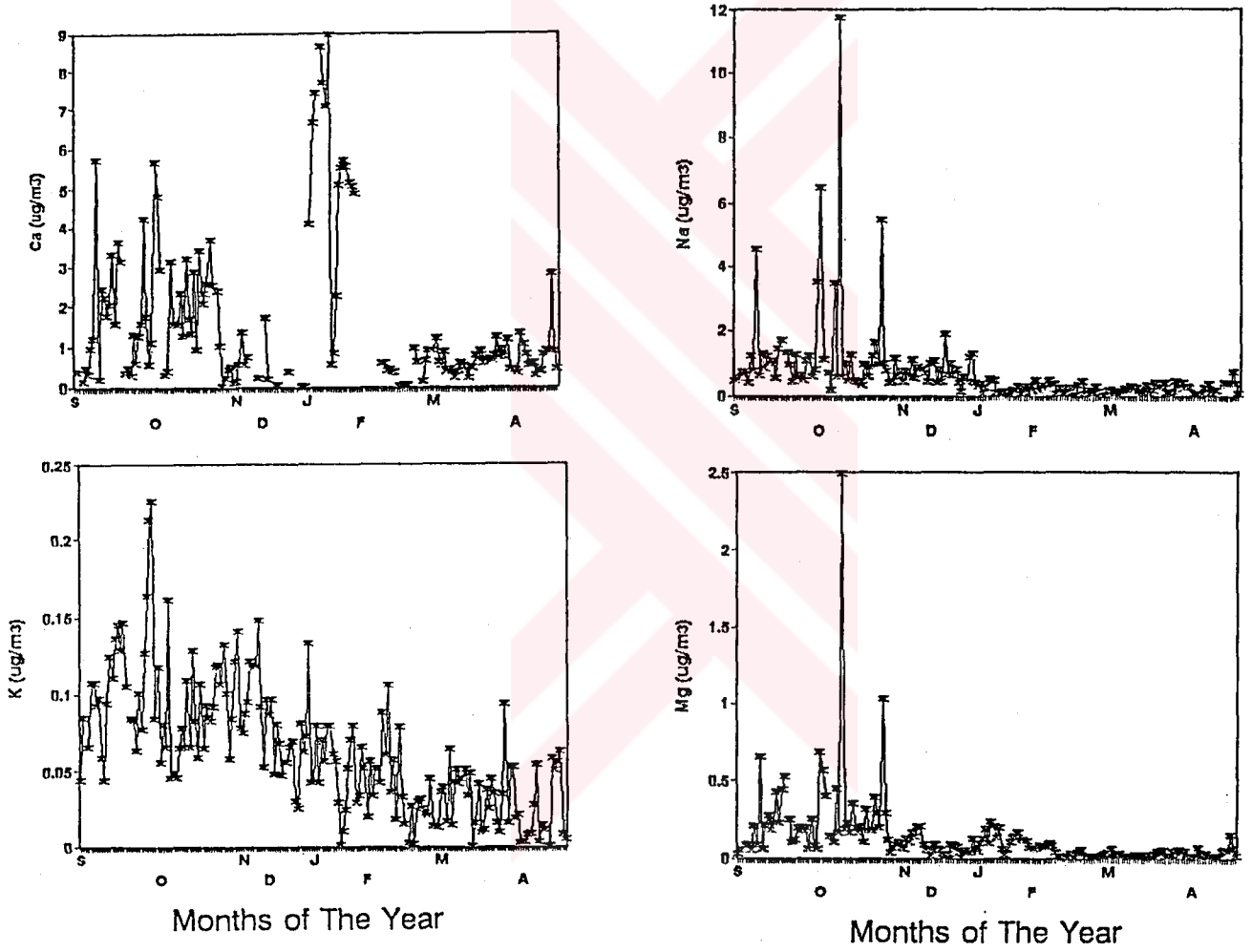

Figure 3.2 Time sequence plots of Ca^{2+}, K^{+}, Na^{+} and Mg^{2+}

Calcium showed some sharp spikes for some days in September, October and in January. In other days it did not fluctuate very much. Contribution of earth crust was high in September and October because of relatively dry weather. But the reason that Ca^{2+} showed spikes in January is questionable. In the same way, magnesium and sodium showed very high fluctuation during dry days as compared to wet days. Potassium always showed spikes over low background concentrations although concentrations were high in dry days. Ammonium ion also fluctuated more and the concentrations were high in dry days and in spring season because of fertilizing process. Sulfate and chloride ions showed spikes in most days of November and December. Nitrate ion fluctuated more in spring season, in few days of February, September and December. High variations from one day to another could be the result of different sources.

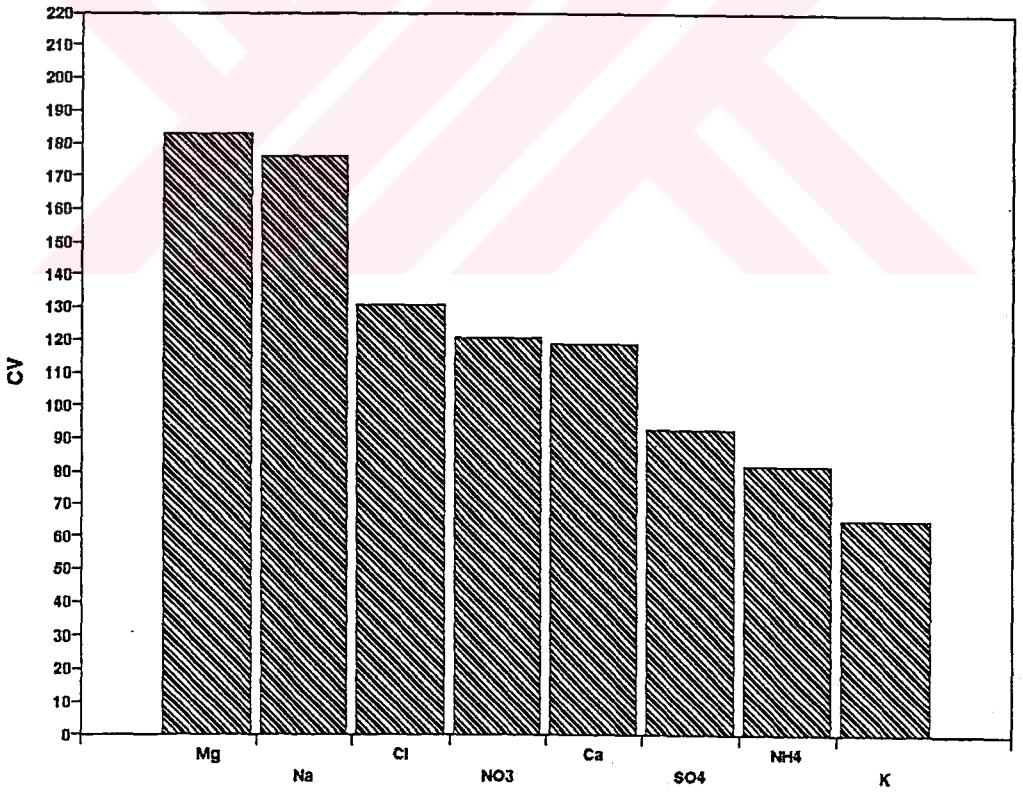

Figure 3.3 Coefficient of variation of ions

affecting the receptor site. In addition, coefficient of variation can explain the degree of fluctuation in the individual ions. One having high coefficient of variation, as term implies, has more concentration variations from one day to another and affected by different sources, as shown in Figure 3.3.

3.2.2. Monthly Variations

Monthly variations of the measured parameters are given in Figure 3.4. Magnesium, sodium and calcium showed high concentrations in September and October. However, Mg, Na and Ca had a higher concentration in October than that of in September. This may be the result of the high wind blown dust in this month. In winter and spring seasons, they showed a significant decreasing trend because of the snow cover that avoided the crustal contribution in these seasons. In November and December together with chloride, concentration of sodium was high. This suggested that besides the crustal source, some part of its concentration might have come from the sea with high northerly wind speeds. Potassium showed regular decreasing trend on a monthly basis. In September and October, since they are dry months, concentration of potassium might also have been increased from the biomass burning besides the crustal contribution. In other months, there was small contribution of the crustal and biomass burning due to the wet weather conditions. Sulfate had higher concentrations in September, October, November and December than in January, February, March and April. In the first group of months sulfur dioxide, SO_2, had lower concentrations because of no residential heating. This first period with an average temperature of 6.8 ^{o}C, was warmer than the second period with an average temperature of -2.8 ^{o}C as shown in

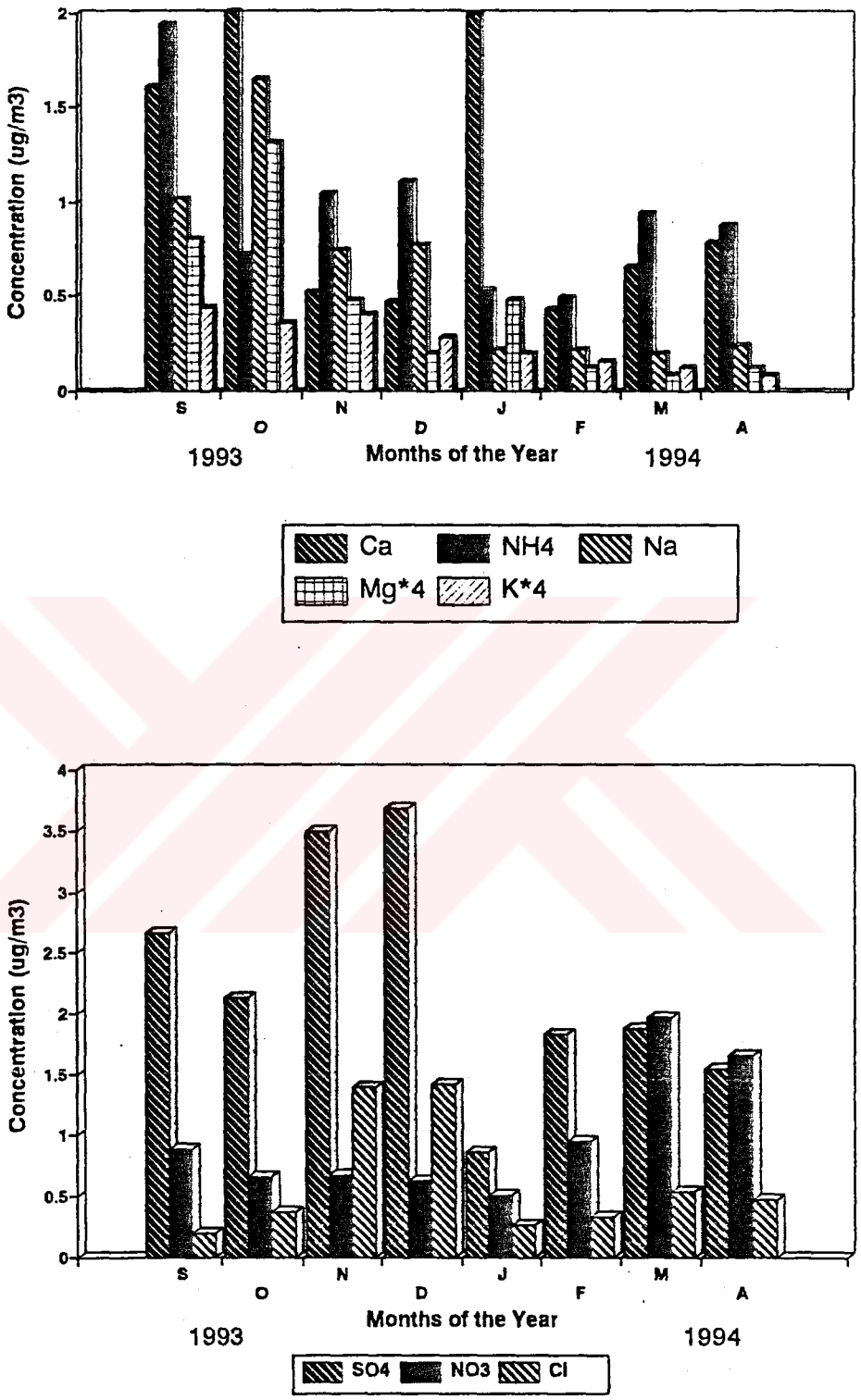

Figure 3.4 Monthly variations of ions

Figure 3.5. Solar flux in the first period was also higher and so photochemical oxidation of SO_2 was little enhanced as shown in Figure 3.6. Additionally high SO_2 concentrations in January, February, March and April is the result of high fresh contribution of Orhaneli power plant which was operating in that period. In November and December, sea salt contribution may be effective. Concentration of NH_4^+ ion showed an increase in the autumn season and a slight increase in the spring season due to the fertilizing process. In the warmer period (including autumn), temperature will increase the emissions of ammonia from the ground surface, may be neutralized more by acidic aerosols [38]. Temperature effects on the equilibrium and kinetic parameters of important atmospheric conversion reactions could be important phenomena [6]. Another NH_3 sources may be anthropogenic, from the decomposition of large amount of urban wastes and fertilizers or it may be emitted through biomass burning and animal wastes. Chloride had high values in November and December. Sea salt contribution in these months was high due to high wind speeds which is not allowing the evaporation of chloride during the transportation from sea to the sampling site. In January and February, sea salt contribution was lower but the contribution of automobile emissions which might be coming from the nearby road to the ski resort area was significant. Again in March and April it had a marginal increase in concentration, this time most probably both sea salt and automobile emissions were important sources. Nitrate had high average concentration in March and April. This result could be due to primary particulate NO_3^- or high HNO_3 concentrations in the atmosphere.

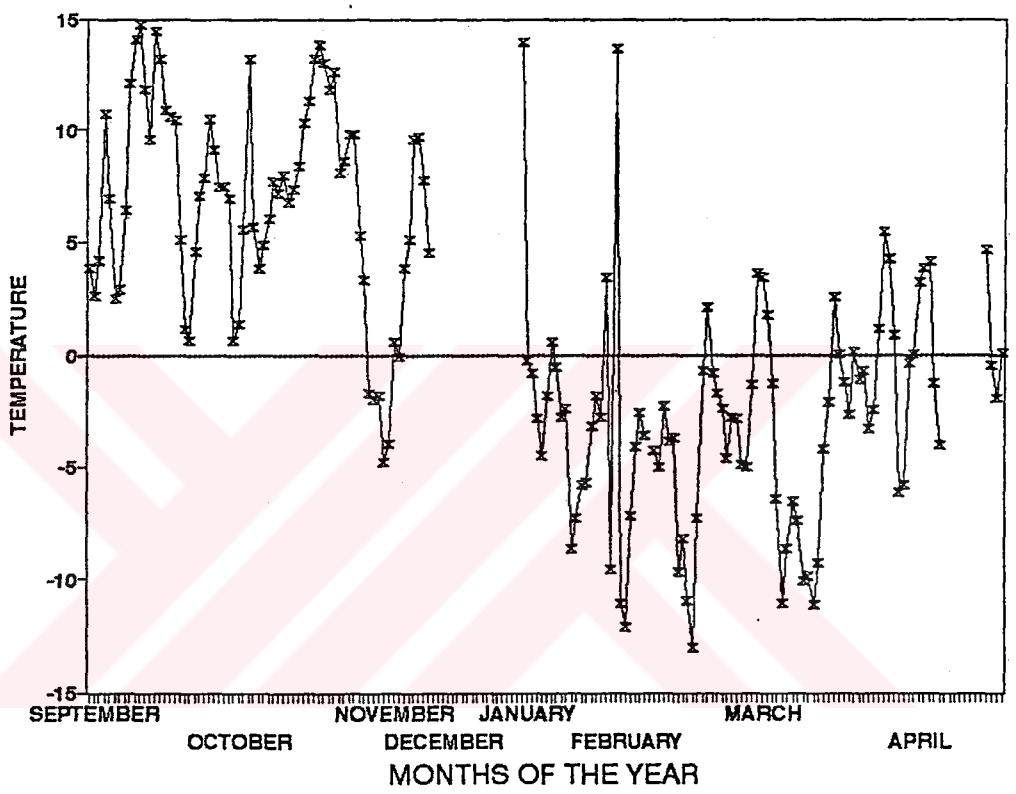

Figure 3.5 Daily temperature variations

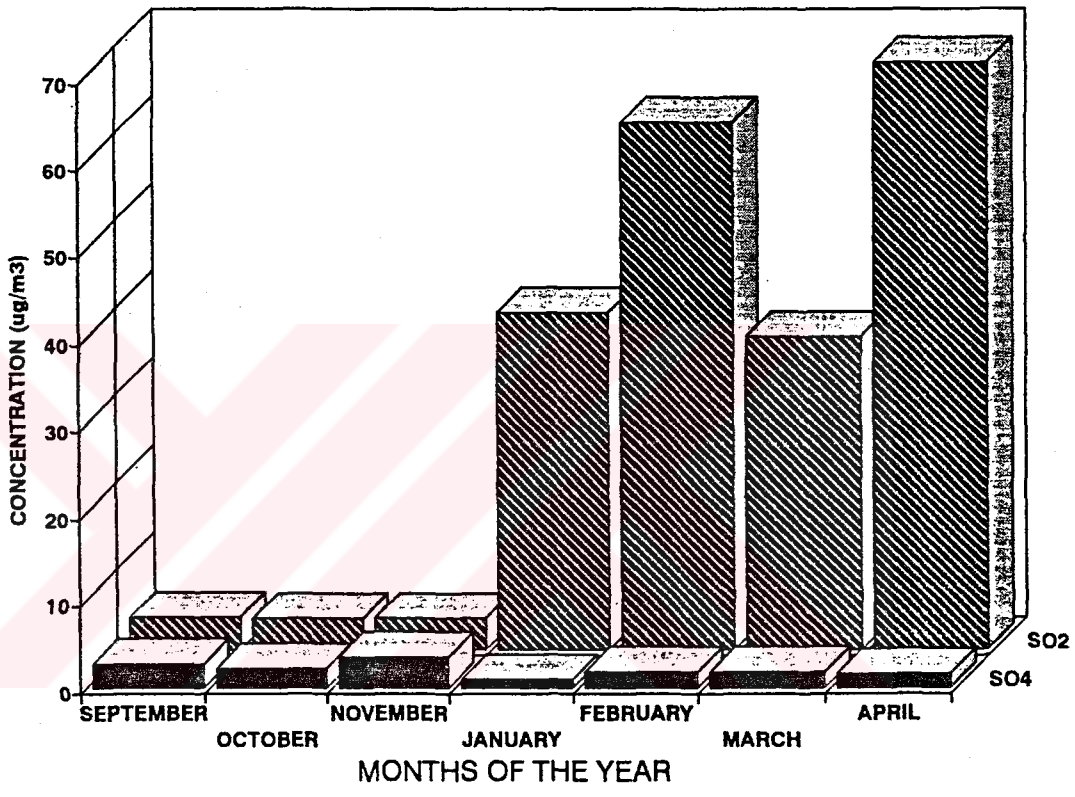

Figure 3.6 Monthly concentration changes of SO_2 and SO_4^{2-}

3.3. Base-line Averages

The average base-line concentrations of ions were calculated by excluding spikes from the data set. Base-line concentrations of ions can be considered as a regional background and also it gives an idea about the anthropogenic emissions. Larger the difference in between base-line and normal average concentration is the larger possibility of anthropogenic contribution. Table 3.3 is given to compare the base-line concentration averages with normal concentration averages. In order to support the idea that our base-line concentrations reflect the regional background concentrations, we can only compare our data with Antalya and Black Sea normal average aerosol concentration data. By comparing these data with our work, we can say that our base-line concentrations are representative of regional background concentrations.

Since the average normal concentration to base-line concentration ratio of Cl^-, NO_3^-, SO_4^{2-}, NH_4^+ and Ca^{2+} are very high, background concentrations were increased by anthropogenic emissions. Concentration of chloride may be increased by both marine contribution and automobile emissions. Concentration of SO_4^{2-} possibly was affected by long range transport and the photochemical conversion of SO_2 coming from fossil fuel or coal burning to SO_4^{2-}. Concentration of NH_4^+ can be mostly affected from the fertilizers as in the form of $(NH_4)_2SO_4$ and NH_4NO_3 particles and then ammonium particles can escape to the atmosphere, both as NH_3 and particulate forms. In the air NH_3 neutralizes strong acids and turn to again particulate forms. Anthropogenic sources of nitrate can be first photochemical conversion of NO_x coming from automobile emissions and fossil fuel burning to NO_3 and second gaseous HNO_3. The composition of

other ions Mg^{2+}, Na^{+}, K^{+} were dominated from the crustal sources, so anthropogenic contribution was not so effective.

Table 3.3 Comparison of base-line concentrations with overall concentrations.

Ions ($\mu g/m^3$)	Base-line Conc.			Measured Conc.			
	Average	Standard Deviation	N	Average	Standard Deviation	N	Ratio
Cl^-	0.13	0.08	54	0.47	0.61	158	3.6
NO_3^-	0.44	0.37	55	1.00	1.21	168	2.3
SO_4^{2-}	0.68	0.47	37	2.15	1.99	172	3.2
NH_4^+	0.38	0.33	39	1.02	0.83	150	2.7
Mg^{2+}	0.09	0.07	39	0.12	0.22	180	1.3
Na^+	0.38	0.35	53	0.67	1.18	174	1.8
K^+	0.04	0.02	51	0.06	0.04	178	1.5
Ca^{2+}	0.46	0.36	37	1.61	1.91	145	3.5

N: Number of samples.

3.4. Source Apportionment of The Ions

3.4.1 Examining Some Ratios As Source Indicators

The ambient air ratios of some species can be used to find out their sources. In addition ratios can show chemical transformations, chemical composition and proportional contribution of species in the chemical composition of the ambient atmosphere. If we look at the elemental ratios, we assume that element to element source ratios are conserved during the transportation and they represent only one source. However the ratio may not be so conservative due to high volatility of elements and for one of the element it can be more than one contributing source as in the case of chloride to sodium ratio.

Chloride to sodium molar ratio fluctuated more one day to another. Although average molar ratio was 0.9 and sea salt ratio is 1.18 [39]. However the most of the data (70 %) below the sea salt composition ratio. There is a deficiency of Cl^- ion, as it can be lost to the atmosphere as HCl from reaction with strong acids such as HNO_3 and H_2SO_4 forming volatile HCl. Another reason is an increase of Na^+ ion from soil dust sources [40]. But, there is an excess of Cl^- in some samples which might be due to emissions from motor vehicles. The observed Mg^{2+} and Na^+ concentrations in aerosols are generally affected by both sea and dust particles. Marine contribution to elements can be supported by a regression line between ($Mg^{2+}+Na^+$) against Cl^- with a correlation coefficient of 0.72 as shown in Figure 3.7.

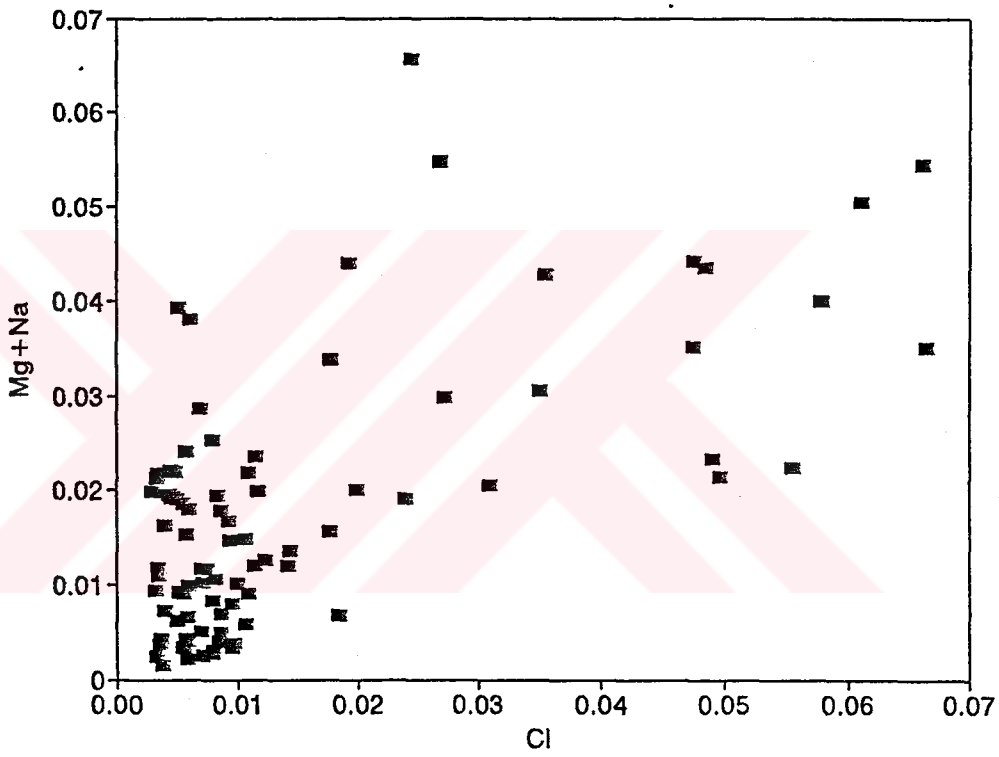

Figure 3.7 Regression plot of (Mg^{2+}+Na^{+}) versus Cl^{-}

Sulfur dioxide to sulfate molar ratio and NO_x to nitrate molar ratio were investigated in order to understand whether the oxidation of SO_2 and NO_x were high or not. As a result they have showed some cycles. Then, we examined their ratio changes with the temperature, SO_2/SO_4^{2-} ratio and NO_x/NO_3^- ratio have showed a decreasing trend with the temperature. In order to see the temperature effect clearly, concentrations of all four species were plotted against the temperature individually. As shown in Figure 3.8 and in Figure 3.9, SO_4^{2-} and NO_3^- had a slight increasing trend whereas SO_2 and NO_x had a slight decreasing trend with the temperature. These were expected results, as the gas phase photochemical conversion of SO_2 and NO_x to SO_4^{2-} and NO_3^-, respectively, were higher in summer or in warm weather than in winter or cold weather, since both the solar intensity and the length of day were reduced in winter. Considering the chemical transformations, seasonal variation in the solar intensity seems to be a dominant factor since the most atmospheric chemical processes are photochemically produced, either by directly or by intermediates [6]. The effect of solar intensity is also important for aqueous phase reactions, since the cold season concentrations of photochemically produced soluble oxidants such as H_2O_2 is lower than the warm season [41,42,43]. Some individual concentrations and concentration ratio changes with warm and cold periods are shown in the Table 3.4. In the warm period SO_2/SO_4^{2-} ratio was very small compared with the cold period, again due to the high emissions of SO_2 in cold period and faster conversion of SO_2 to SO_4^{2-} in the warm period. NO_x/NO_3 ratio did not show a remarkable change in both periods. This was the result of their parallel concentrations changes in two periods and photochemical conversion is more important mechanism of

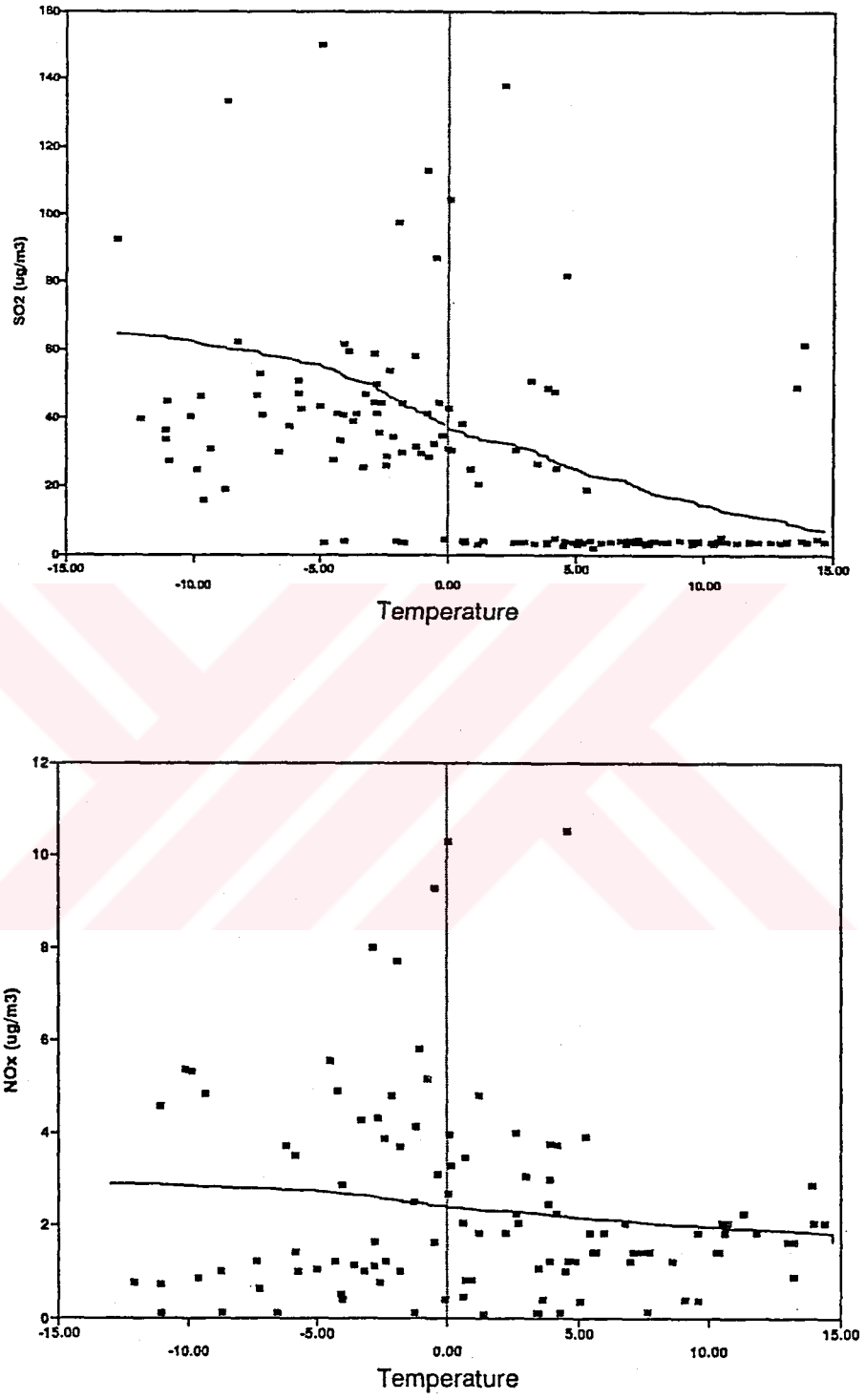

Figure 3.8 Variation of SO_2 and NO_x with the temperature

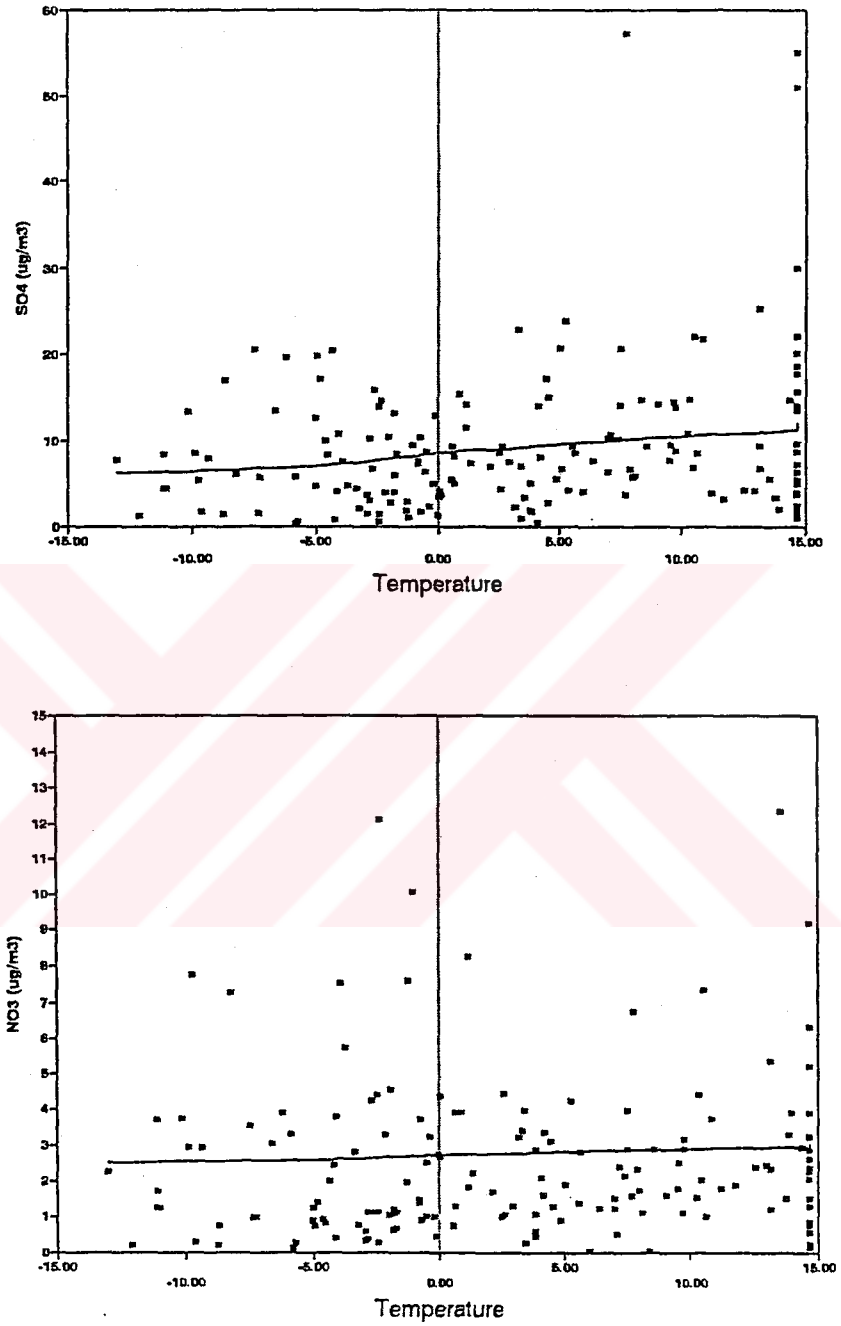

Figure 3.9 Variation of SO_4^{2-} and NO_3^- with the temperature

Table 3.4 Average warm and cold period parameters.

Concentrations ($\mu g/m^3$)	Warm Period		Cold Period	
Parameter	Average	Standard Deviation	Average	Standard Deviation
Temperature	6.8 ^oC	4.6^oC	-2.7^oC	4.9 ^oC
NO_x	1.42	0.67	3.00	2.44
SO_2	3.70	0.52	61.6	60.8
NO_3^-	0.73	0.59	1.25	1.53
SO_4^{2-}	2.80	2.43	1.58	1.22
TSP	15.9	7.51	36.8	56.1
Concentration Ratios				
SO_2/SO_4^{2-}	2.15	1.53	72.6	127
NO_x/NO_3^-	5.64	19.2	6.05	9.60
SO_4^{2-}/NO_3^-	4.96	2.67	2.91	2.53
$SO_4^{2-}/(SO_2+SO_4^{2-})$	0.29	0.13	0.024	0.021
$NO_3^-/(NO_x+NO_3^-)$	0.29	0.18	0.23	0.21
SO_2/TSP	0.30	0.16	4.42	3.32

conversion of NO_x to NO_3^-.However, from these ratio changes, it is inferred that photochemical conversion may not explain alone the relation between the gaseous precursors and particulate NO_3^- and SO_4^{2-}.

The equivalent ratio of SO_4^{2-}/NO_3^- indicates the relative contributions of SO_4^{2-} and NO_3^- ions to the aerosol acidity. However we are not considering the organic acids which may constitute 30 % of total acidity in aerosol samples [44,45]. This ratio was reported to be approximately about 3.0 in rain water [46]. However in this research it was around 5.0 in the warm period which means that contribution of H_2SO_4 was very high compared with HNO_3 to aerosol acidity. The ratio was approximately 3.0 and it was similar to the literature value in the cold period. The ratio was decreased because of the increased NO_3^- ion concentration in that period.

The fraction of $SO_4^{2-}/(SO_2 + SO_4^{2-})$ was calculated and averaged to be 0.16. The plot of daily variation of the fraction is given in Figure 3.10. The fraction was generally lower during the periods of high SO_2 concentrations, as it is mentioned before, suggesting additions of fresh SO_2 emissions sources widely distributed around the sampling site especially from the Orhaneli power plant which was operating in the periods of high SO_2 concentrations and also from the domestic heating to background SO_4^{2-} concentrations and it was higher during warm period due to lower SO_2 emissions from the domestic heating as illustrated in Figure 3.6. The average value is very small to explain that SO_4^{2-} concentrations mainly come from the conversion of SO_2 to SO_4^{2-}. In addition the fraction of $NO_3^-/(NO_x + NO_3)$ was averaged 0.33 which was also small value. The conversion rate depends on both OH· radicals and H_2O_2 and O_3 oxidants in the air. It may be as low as 0.2 % hr^{-1} in winter and as high as 1-4 % hr^{1}

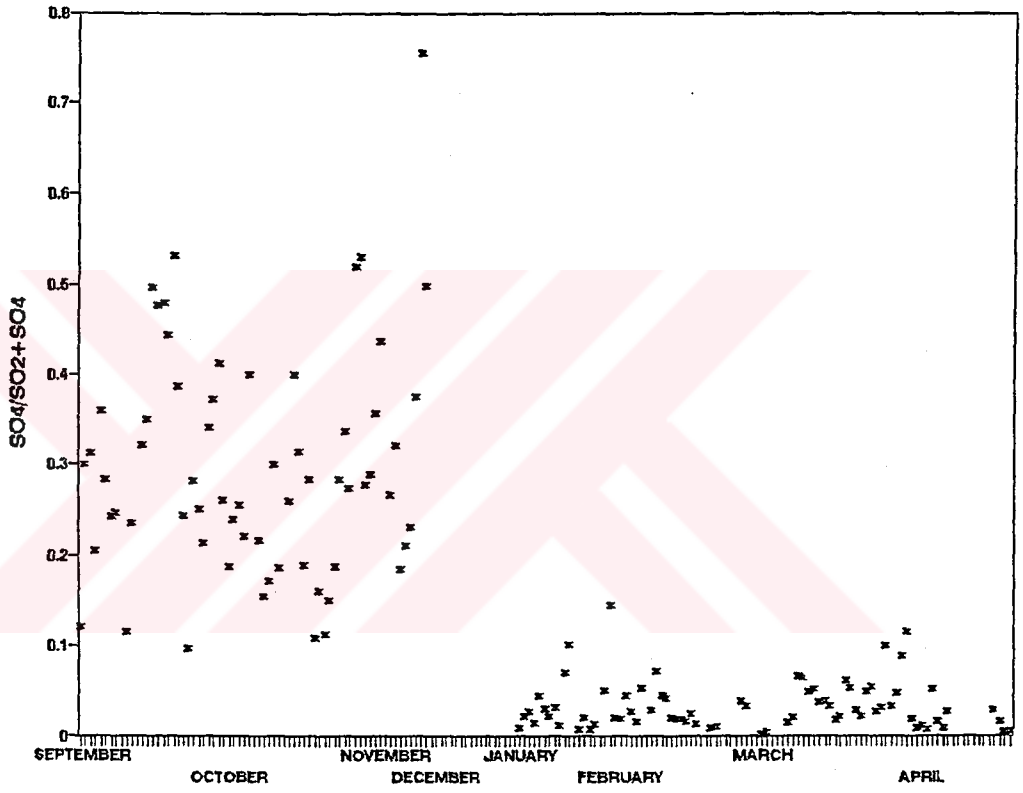

Figure 3.10 Daily variation of $SO_4^{2-}/(SO_2+SO_4^{2-})$ fraction

in summer [42]. The distance between the sampling site and source of SO_2 and wind speed are important parameters to calculate the approximate conversion rate. From these calculations it was understood that approximately 3-6 % of SO_2 was converted to SO_4^{2-} from the possible sources. These results suggest that particulate NO_3^- and SO_4^{2-} was the result of the long range transport. Long range transport give an idea about the pollutants coming with the clouds passing over the source regions so we can understand how effective pollutants coming with these clouds to the sampling site and how effective the local pollutants. Therefore the effect of long range transport was important to our sampling site. Concentrations of SO_2 and TSP were high in the second period, however concentration of SO_2 had a higher increase than that of TSP. So the ratio of SO_2/TSP was increased in the second period. Since they show the similar behaviour they might be emitted from the same source.

Figure 3.11 shows a comparison between the microequivalents of NH_4^+ ion and the sum of the μeq of NO_3^- and SO_4^{2-} ions. A linear regression between these species had a correlation coefficient of 0.44. It seemed that ammonium ion did not neutralize the H_2SO_4 and HNO_3 aerosols completely. Average ratio of $NH_4^+/SO_4^{2-}+NO_3^-$ was 1.5. This ratio also confirmed that most of the SO_4^{2-} and NO_3^- ions were not present as an ammonium salt.

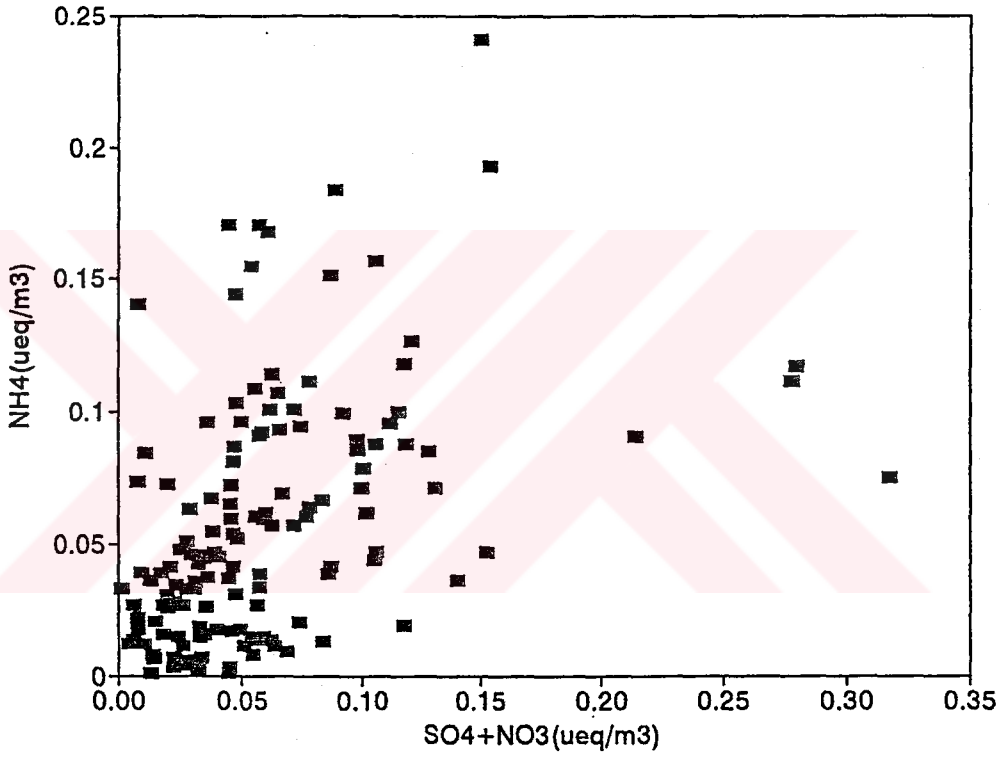

Figure 3.11 Scatter plot of NH_4^+ versus $SO_4^{2-}+NO_3^-$

3.4.2. Ion Balances

Scatter graph of the sum of anions and the sum of cations are shown in Figure 3.12. The correlation between them is moderately good (r=0.43) and cation to anion ratio was averaged 1.44. Cation excess was seen clearly. Concentration of hydrogen ion, HCO_3^- ion and organic anions were absent in our work. It is demonstrated that in precipitation organic acids by direct emission from the forest canopy such as formic and acetic acids account for about one half of the total anion equivalents [47] and organic acids also constitute a significant portion of the atmospheric aerosol. One study estimated that approximately 30 % of the ether-extractable compounds in the aerosol are organic acids [44]. These acids also have anthropogenic sources such as products of fuel combustion especially from automobile emissions and also from fuel additives [40].

3.4.3. Correlations of Ions in The Aerosols

Binary correlations between measured ions were computed in order to obtain additional information on the sources of ions in the aerosol samples. If concentrations of two ions fluctuate in the same manner from sample to sample, they have good correlations (high correlation coefficient value), and they are said to have common sources. Binary correlation coefficients of ions are given in the Table 3.5. Generally, ions are not strongly correlated to each other, since different sources affect the sampling site. Only Ca^{2+}, Mg^{2+} ions are strongly correlated due to their common crustal source. Magnesium ion is also correlated with K^+ ion. Sodium, Cl^- and SO_4^{2-} are correlated to each other indicating that certain fractions of

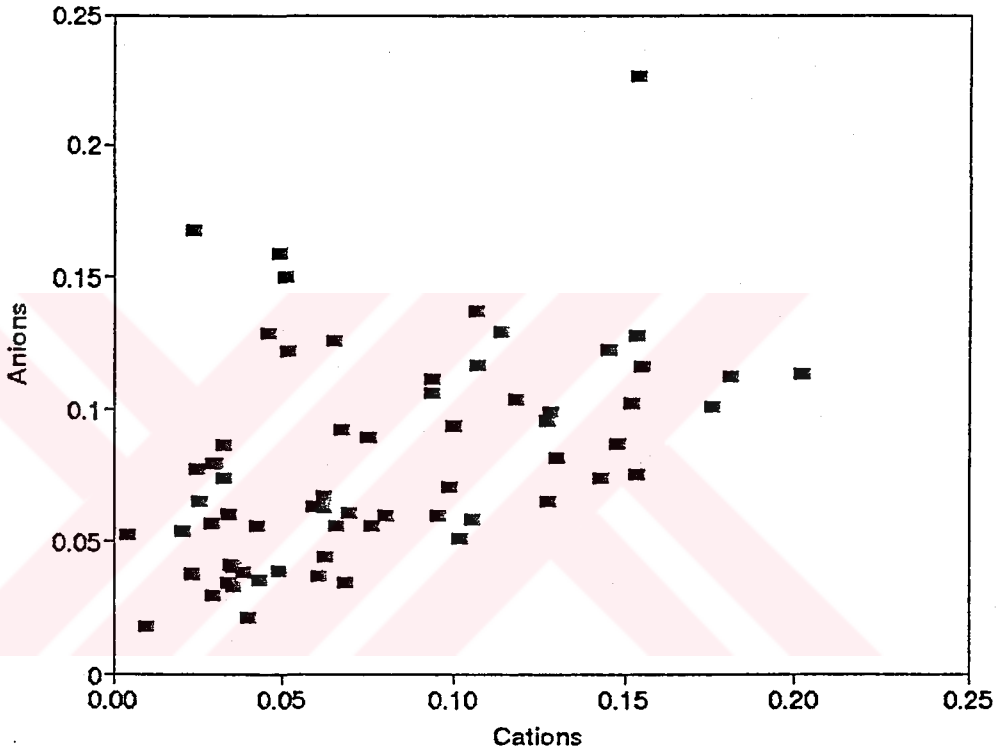

Figure 3.12 Regression graph of anions and cations in aerosol samples

Table 3.5 Binary correlation coefficients between ions in aerosol.

	Cl^-	NO_3^-	SO_4^{2-}	Mg^{2+}	Na^+	K^+	Ca^{2+}	NH_4^+
Cl^-	1.00							
NO_3^-	-0.03	1.00						
SO_4^{2-}	0.52	0.16	1.00					
Mg^{2+}	0.18	-0.15	0.15	1.00				
Na^+	0.56	-0.01	0.37	0.31	1.00			
K^+	0.42	0.06	0.54	0.60	0.63	1.00		
Ca^{2+}	-0.15	-0.21	-0.21	0.81	- 0.12	0.24	1.00	
NH_4^+	0.10	0.18	0.43	-0.06	0.20	0.30	-0.20	1.00

them can be accounted for by sea salt. Potassium ion is also correlated with Na^+ ion. Sulfate, NH_4^+ and K^+ ions are correlated to each other although they do not give high correlation coefficient. This may be due to the biomass burning or animal wastes. Sodium chloride, $(NH_4)_2SO_4$, NH_4HSO_4 are predominant species in aerosols. The H_2SO_4 formed can react with the alkaline NH_3 gas to yield $(NH_4)_2SO_4$ and NH_4HSO_4 but the presence of NH_4HSO_4 is relatively small [10].

3.4.4. Multiple Linear Regression

In order to understand an acid-base chemistry in aerosol, a multiple linear regression was applied to SO_4^{2-} and NO_3^- separately using Ca^{2+}, Mg^{2+} and NH_4^+ as independent variables. The coefficients, residues and partial correlation coefficients for all data are given in the Table 3.6. Although we had low r^2 values, we found % of r^2 explained by individual ions. In total 38 % of SO_4^{2-} and 11 % of NO_3^- were explained by Ca^{2+}, Mg^{2+} and NH_4^+. Out of this 38 %, 25 % of SO_4^{2-} concentration was neutralized by $CaCO_3$ and remaining part was neutralized by NH_3. For NO_3^- ion 8 % out of explained 11 % was explained by $CaCO_3$, 40 % of it was neutralized by NH_3 and the remaining 52 % was neutralized by $MgCO_3$. From this feature, two things can be said: First one is that the neutralizing species for these two anions are different. Second one is that an approximately 60 % of H_2SO_4 and 90 % of HNO_3 were not neutralized by these bases. This result could be explained by the presence of a stable organic film on aerosol particles which may inhibit neutralization, due to the possible formation of a crystalline salt layer. That is a frequently observed situation for the aerosols collected on forest area [39].

Table 3.6 Multiple linear regression parameters for SO_4^{2-} and NO_3^- ions regressed against Ca^{2+}, Mg^{2+} and NH_4^+.

Sulfate		$[SO_4^{2-}] = a + \alpha_1[Ca^{2+}] + \alpha_2[Mg^{2+}] + \alpha_3[NH_4^+]$	
a	0.81	r^2	0.38
α_1	0.20	% of r^2 explained by Ca^{2+}	25
α_2	5.51	% of r^2 explained by Mg^{2+}	0
α_3	0.94	% of r^2 explained by NH_4^+	75
Nitrate		$[NO_3^-] = b + \beta_1[Ca^{2+}] + \beta_2[Mg^{2+}] + \beta_3[NH_4^+]$	
b	1.04	r^2	0.11
β_1	-0.07	% of r^2 explained by Ca^{2+}	8.0
β_2	-4.90	% of r^2 explained by Mg^{2+}	52
β_3	-0.02	% of r^2 explained by NH_4^+	40

3.4.5. Enrichment Factors of Elements

Enrichment factors (EF) is the first step in source apportionment of atmospheric pollutants. It is a double normalization technique in which the elemental composition of the local ambient aerosol is compared with the elemental composition of the possible sources. In this work we have used Ca as an indicator element of the earth crust. EF values are calculated by using the following formula:

$$(EF)_{source} = \frac{(C_i/C_n)_{sample}}{(C_i/C_n)_{source}}$$

where C_n is the concentration of normalizing element assumed to be characteristics of the source and C_i is the concentration of an element whose enrichment is to be determined [48].

Mean enrichment factor, standard deviation and ranges of EF values are listed in the Table 3.7.

If EF is around unity for the test element, one can assume that this element is entirely from the source used in calculations. Elements with enrichment factors greater than 10 are assumed to be due to sources other than the background contribution in that receptor site. Mason's compilation for crustal abundances was used in crustal enrichment factor calculations. According to the calculations, only Cl is considered to be highly enriched element and it has other contribution sources in the atmosphere

Table 3.7 Some statistical parameters of EF.

Element	Mean EF	SD	Range
Cl	573	1690	0.14-13000
Mg	0.34	1.39	0.005-12
Na	2.46	10.15	0.001-88
K	0.28	1.14	0.002-10

different than the earth crust. Magnesium, Na, K, are originated from the earth crust. Potassium has some spikes in the enrichment values possibly from the biomass burning. Magnesium and Na sometimes have the EF values greater than 10 indicating some sea salt contribution. Since we have used Ca which may have marine contribution, as a reference element, we got smaller EF values than expected for Mg, Na and K. The best reference element for crust is aluminum but we did not measure Al. Therefore these EF values gave us an overall picture about the enrichment with respect to earth crust.

3.5. Effect of Wind Speed and Wind Direction

Meteorological parameters affect the chemical properties of constituents in the atmosphere. Wind speed is one of them which may change the concentrations of pollutants by diluting them. Variation of concentration with wind speed was investigated in this work. The effect of daily averaged wind speed on the ambient levels of some of the species

such as SO_4^{2-}, Mg^{2+} and NO_x are given in Figure 3.13. It was seen that with high wind speeds, concentrations of gaseous species, ions in aerosol and TSP were decreased. It was clear that the high wind speeds acted as a diluting factor for the concentrations in the atmosphere. Almost 41 % of Uludağ winds blow at a speed between 1 and 2 ms^{-1} and approximately 5 % has speed higher than 6 ms^{-1}. Therefore low wind speed is the characteristics of Uludağ Mountain as shown in Figure 3.14.

Wind direction is another important meteorological parameter which affect the concentrations of measured species. The fifteen minute wind direction data is treated for each day to determine the dominant sector. Each wind sector is named for each 45 degree. Therefore, the most frequently observed wind sector for each day is the representative wind sector of that day. In the case of no directional dominance of a specific wind sector within a day, the sector which has a higher wind speed is chosen. Six hour data for 24 hour period was treated in order to obtain a general wind pattern of Uludağ Mountain. Sectors are assigned setting 0^o as north and 180^o as south. We have defined 16 sectors to represent

N: North	S: South
NNE: North to North East	SSW: South to South West
NE: North East	SW: South West
ENE: East to North East	WSW: West to South West
E: East	W: West
ESE: East to South East	WNW: West to North West
SE: South East	NW: North West
SSE: South to South East	NNW: North to North West

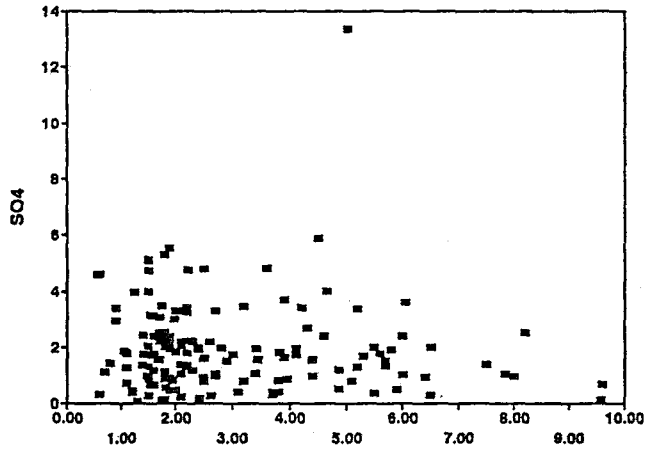

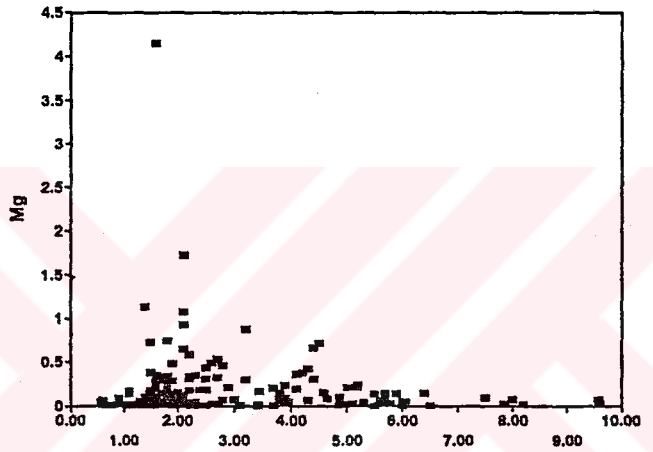

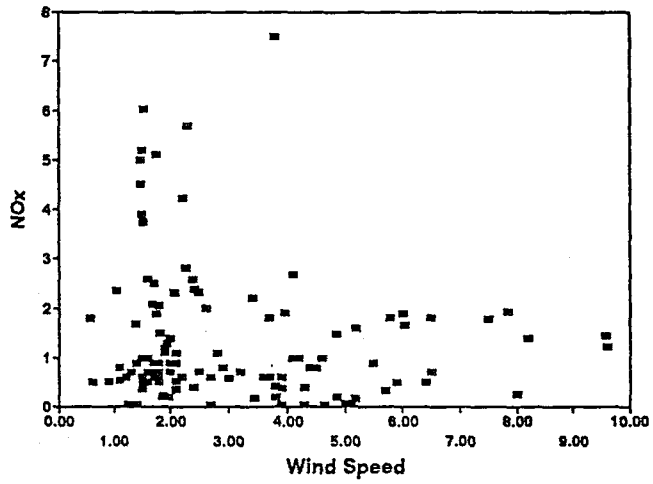

Figure 3.13 Wind speed versus SO_4^{2-}, Mg^{2+}, NO_x concentrations

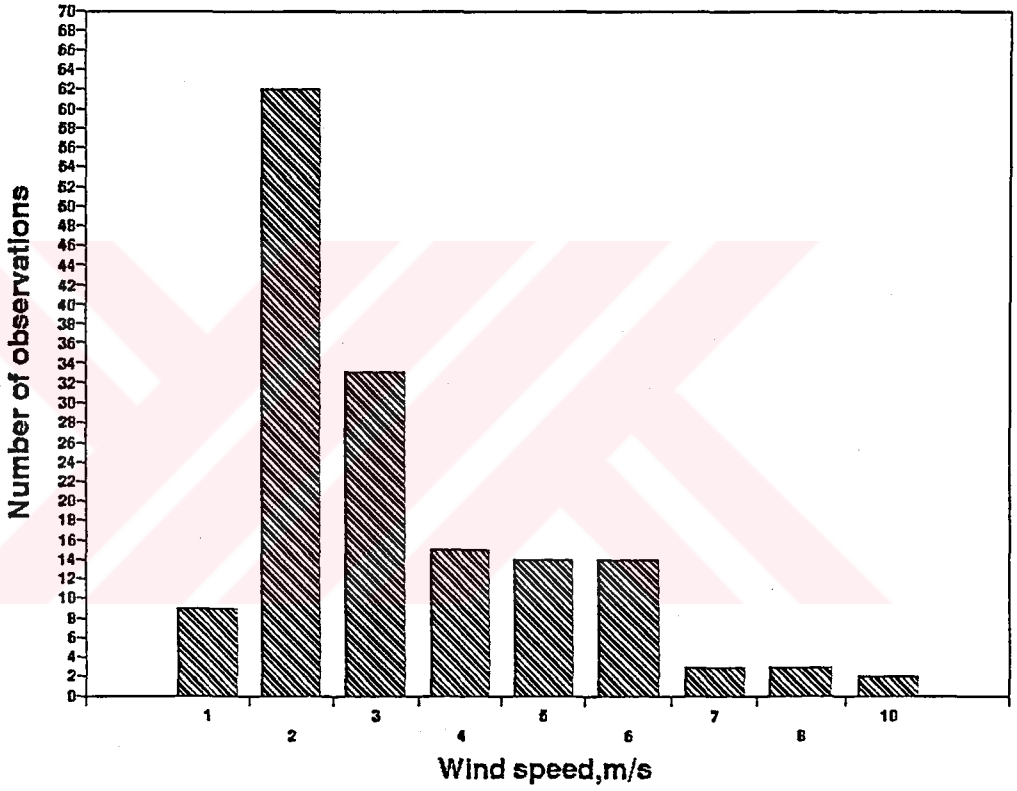

Figure 3.14 Frequency histogram of the wind speed

different wind direction. Wind sector identification and general wind pattern in Uludağ Mountain is given in Figure 3.15.

Although the wind direction changes in one day, most of the time it blows mostly from S, SSE, SSW, N, NNW, NNE directions as shown in the wind rose of Uludağ Mountain. In a typical day almost 85 % of the winds blows from southerly direction and 15 % of the winds from northerly directions. In order to determine the significant source region, average concentration of each parameter in each sector were taken and tabulated in the Table 3.8. Most of the samples were shared by three sectors namely S, SSE, SSW. The highest average concentration of Cl^-, NO_3^-, SO_4^{2-}, Mg^{2+}, Na^+, K^+ came from the north where the contribution of sea, town of Bursa and industrial emissions are effective. Ammonium had its highest average concentration from the wind sector NNE which shows the main agricultural areas and thus intense fertilizing activity in that sector. Calcium and TSP had the highest average concentration at the wind sector SSE and S respectively. Ski resort area and coal-fired power plant in these sectors were the contributors. This combined effect of two sources was seen for the gas phase pollutants SO_2 and NO_x. There exist a potential source region at the southerly and northerly sectors. However, the extend of their contributions is an important question.

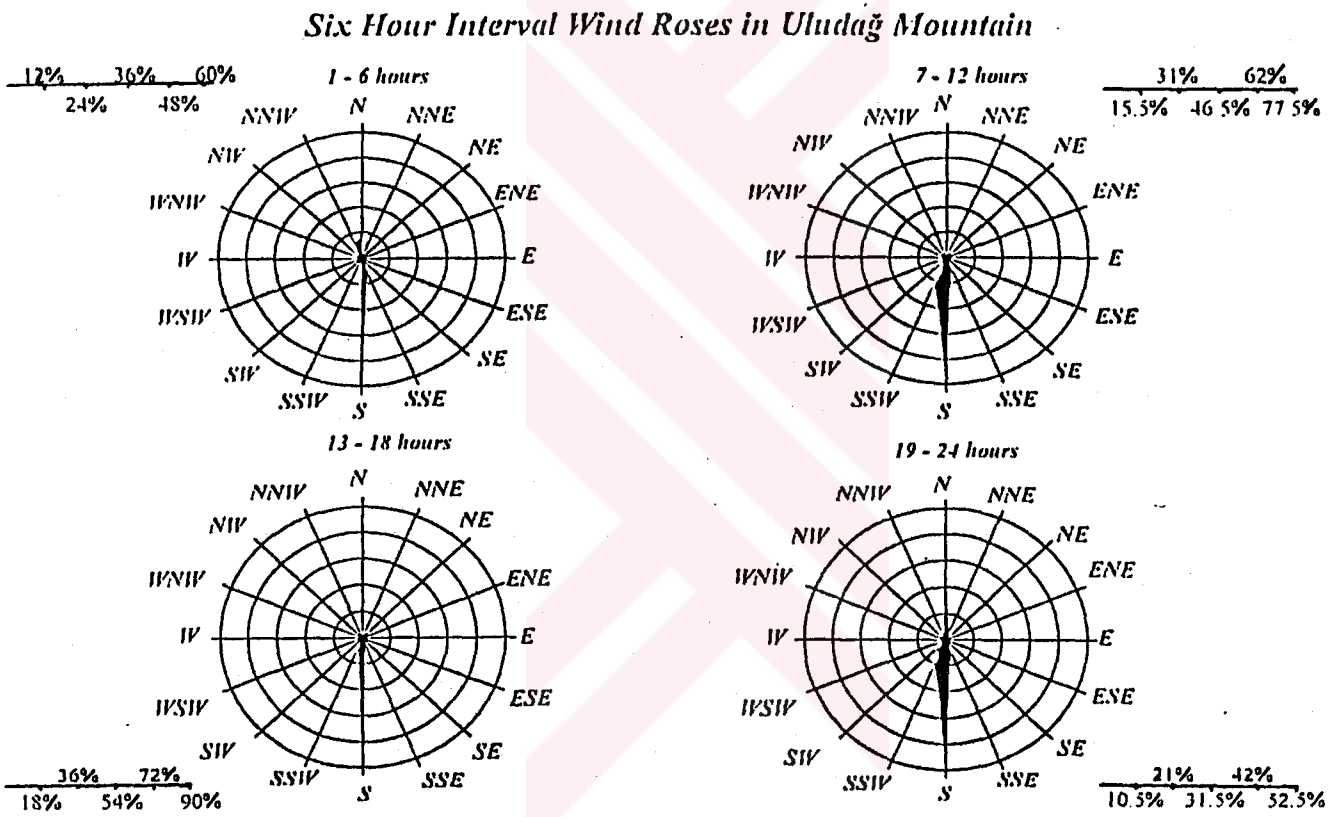

Figure 3.15 General wind pattern of Uludağ Mountain

Table 3.8 Average concentrations of measured parameters from different wind sectors.

	Measured Parameters($\mu g/m^3$)										
Wind Direction	Cl^-	NO_3^-	SO_4^{2-}	NH_4^+	Mg^{2+}	Na^+	K^+	Ca^{2+}	TSP	SO_2	NO_x
NNW	0.14±0.09 (2)	0.37±0.35 (3)	0.84±0.37 (3)	0.66±0.26 (2)	0.09±0.06 (4)	0.53±0.31 (3)	0.05±0.04 (4)	1.3±0.68 (4)	10±8.5 (4)	20±20 (4)	0.88±0.35 (3)
N	1.0±0.89 (5)	1.2±0.68 (5)	5.0±4.3 (5)	1.8±0.98 (5)	0.15±0.07 (4)	0.83±0.09 (4)	0.12±0.04 (5)	1.1±0.95 (2)	16±4.8 (5)	3.5±1.2 (5)	1.1±0.82 (5)
NNE	0.11	1.2±0.74 (2)	4.2±1.8 (2)	3.3±0.20 (2)	0.26±0.17 (2)	0.86±0.21 (2)	0.13±0.02 (2)	1.9±1.4 (2)	12±1.98 (2)	3.4±0.57 (2)	1.8±0.20 (2)
SSE	0.33±0.33 (28)	0.94±1.1 (30)	1.5±1.1 (31)	0.82±0.61 (32)	0.09±0.07 (34)	0.34±0.28 (34)	0.05±0.03 (33)	2.6±2.9 (28)	29±70 (33)	35±25 (34)	2.8±1.8 (29)
S	0.31±0.36 (71)	1.2±1.5 (76)	1.8±1.2 (77)	0.82±0.71 (63)	0.13±0.31 (79)	0.60±1.5 (76)	0.05±0.04 (78)	1.3±1.5 (65)	33±37 (78)	50±69 (73)	2.5±2.3 (52)
SSW	0.41±0.51 (27)	0.82±0.61 (29)	2.5±1.5 (29)	1.4±0.92 (24)	0.21±0.17 (31)	1.2±1.3 (31)	0.09±0.05 (31)	1.8±1.5 (30)	15±7.4 (31)	9.4±20 (32)	1.8±2.0 (20)

Numbers in parenthesis show the number of measurements.

The percent contribution of each wind sector to the observed concentrations was determined by the procedure used by the Vossler et al. [49] and are given in the Table 3.9. This contribution to each parameter k from each wind sector j is calculated as

$$[C_{kj}]/[C_k]*F_j = 1/N\ \Sigma([C_{ik}]*F_j)/[C_k]$$

Where, F_j is the frequency of winds from sector j, C_{ik} is the concentration of parameter k for the sampling period i, C_{kj} is the average concentration of parameter k from wind sector j, C_k is the average concentration of parameter k in all samples and N is the total number of observations.
Major contributing sector for all parameters is from the southerly direction. This is purely due to very high frequency of winds from this sector. Magnesium, sodium, potassium, sulfate, nitrate had approximately same percentages from the south, but calcium also had the relatively high percentage from SSE direction as compared to the other parameters. This sector also had the highest average concentration of calcium. Ammonium had the largest percentage of NNE sector of all parameters which was again the dominant sector for the average values of NH_4^+. Chloride showed the same behaviour for the north sector which gave the highest average concentration of chloride presenting sea contribution. Contribution of wind sectors on SO_2, NO_x, TSP indicated the significant dominance of southerly winds more clearly. Because the power plant is the main source of these pollutants, one would expect not only high percent contribution from southerly directions, but also high concentrations when the wind blows in that direction. Small frequency of northerly winds resulted in smaller percent contribution.

Table 3.9 Percent contribution of different wind sectors to the observed concentrations.

	Wind Direction					
Parameters	NNW	N	NNE	SSE	S	SSW
Mg^{2+}	3.5	2.8	2.5	14	45	31
Na^{+}	1.6	3.3	1.7	12	45	37
K^{+}	2.1	6.1	2.6	18	43	28
Ca^{2+}	2.3	1.0	1.7	32	39	24
NH_4^{+}	1.0	7.0	5.1	20	40	26
Cl^{-}	0.40	11	0.10	19	46	23
NO_3^{-}	0.70	4.0	1.6	19	59	16
SO_4^{2-}	0.90	8.5	2.8	16	47	25
TSP	1.0	1.9	0.60	23	62	11
SO_2	1.6	0.33	0.13	23	69	6.0
NO_x	1.0	2.0	1.4	31	50	14

3.6. Ambient Concentrations of Ions in Snow and Comparison with Literature Values

Concentrations of ions in snow are given in the Table 3.10. The statistical results include mean, standard deviation, and range. The highest average concentrations were in the order of $H^+ > SO_4^{2-} > Ca^{2+} > Cl^- > NO_3^- > NH_4^+ > Na^+ > Mg^{2+} > K^+$. Snow samples were not collected on event bases, they were bulk samples including wet and dry deposition. Concentrations can be affected by the amount of snow and the amount of dry deposition. Therefore standard deviations of snow samples were high.

When we compare our data with the literature values as shown in the Table 3.11, it is seen that our results are comparable only with the work done in Pylylimon in Great Britain [50] where samples were taken using polypropylene jars to a depth of between 50 and 200 mm below the surface within 3 days or a week. There was an accumulation of black dust particles on the surface of the snow. In our work there was also a dry deposition during one week. Their chloride, potassium, sodium concentrations were high because of marine effect. Other two literature values are comparable to each other but not to our study. The sampling for the first one was done in Washington Cascade at an elevation of 2054 m for one week period [26]. Bulk samples were taken in the polyethylene buckets and it was open to the dry deposition so the effect of dry deposition on the concentrations of the ions is not so much in this work. For the second work, surface snow samples were collected with wet-only sampler during each snow event at the five sites of Mountain in

Table 3.10 Summary of snow concentrations at Uludağ Mountain.

Ions (μeq/L)	Mean	Standard Deviation	Range Min.	Max.
H^+	181	165	0.26	550
Ca^{2+}	52.0	53.8	12.6	162
Na^+	20.6	17.2	0.91	54
K^+	2.35	1.20	0.64	3.9
Mg^{2+}	19.8	15.6	5.84	55
NH_4^+	22.0	21.5	2.26	70
Cl^-	34.0	28.4	6.80	102
NO_3^-	23.9	14.6	10.3	58
SO_4^{2-}	53.0	48.4	17.3	183

Table 3.11 Average levels of major ions in snow in the different parts of the world.

Ions	This work	Plynlimon Great Britain (Rural)	Washington Cascades (Mountain)	California (Mountain)
pH	4.36	3.89		5.7
H^+	181	129	5.1	2.0
Ca^{2+}	52	14	1.1	5.9
Mg^{2+}	20	11	0.7	1.3
Na^+	21	30	4.7	3.0
K^+	2.4	5	0.5	1.1
NH_4^+	22			4.3
Cl^-	34	69	5.6	5.8
NO_3^-	24	64	5.3	10.9
SO_4^{2-}	53	78	3.4	7.6

California [51]. Local pollution sources, and at some extent dry deposition and sources in the immediate vicinity of the station increased the concentration levels in our snow samples.

3.7. Temporal Variations of Ions in Snow

In the Table 3.12, number and date of snow samples, individual concentrations of ions for each sample and cation to anion ratios are given and also temporary variation plots of the some of the ions are shown in Figure 3.16. From these information, it was observed that concentrations of SO_4^{2-}, NH_4^+ and NO_3^- were high in sample 8 together with high H^+ ion concentration. In general sulfate, nitrate and ammonium ions showed similar behaviour in all samples and Na^+, K^+, Mg^{2+} and Ca^{2+} showed similar trend in all samples.

For Na^+, K^+, Cl^-, Mg^{2+}, Ca^{2+} ions, first sample concentrations were high, then in the second sample which was consecutive of the first one, concentrations dropped to the relatively low concentration values. This may be the result of two factors: The first week snow may remove the pollutants and the second sample can only remove what remains or there will be little precipitation which brings little scavenging. After two weeks later, third sample was taken and it contained again high concentrations of same ions since air pollutants were concentrated in the air. Samples 3,4,5,6,7 were consecutive samples. Concentrations showed a decreasing trend in general except for the seventh sample. Third sample was taken after two weeks later than the second sample and concentrations increased again may be due to high loadings of pollutants in the air. Concentrations of these cations

Table 3.12 Concentration and cation/anion ratio changes of ions in snow samples in ueq/L.

Sample No	Date	H^+	Ca^{2+}	Mg^{2+}	Na^+	K^+	NH_4^+	Cl^-	NO_3^-	SO_4^{2-}	(Cat/An)	(Cat/An)*
1	25-31.12.93	234	20.9	10.6	21.3	1.28	---	21.4	10.3	19.2	1.06	5.66
2	1-7.1.94	550	14.4	9.55	9.00	0.639	---	11.8	12.9	39.2	0.526	9.13
3	22-28.1.94	251	44.0	14.3	19.4	3.89	27.3	35.2	37.7	41.0	0.956	3.16
4	29.1-4.2.94	229	34.0	14.3	20.8	2.79	19.6	12.4	17.9	40.6	1.29	4.52
5	5-11.2.94	91.2	12.6	7.65	1.30	---	2.26	6.76	13.7	22.3	0.556	2.69
6	12-18.2.94	28.2	15.5	5.84	0.913	---	10.1	102	15.8	17.3	0.239	0.447
7	19-25.2.94	2.51	26.1	55.2	13.3	1.18	4.21	18.0	22.7	46.7	1.14	1.17
8	12-18.3.94	240	138	22.7	45.3	3.38	70.5	47.3	58.7	183	0.969	1.80
9	2-8.4.94	0.263	162	37.8	53.7	3.33	20.1	51.0	25.6	67.5	1.92	1.93

*Hydrogen ion concentration is included.

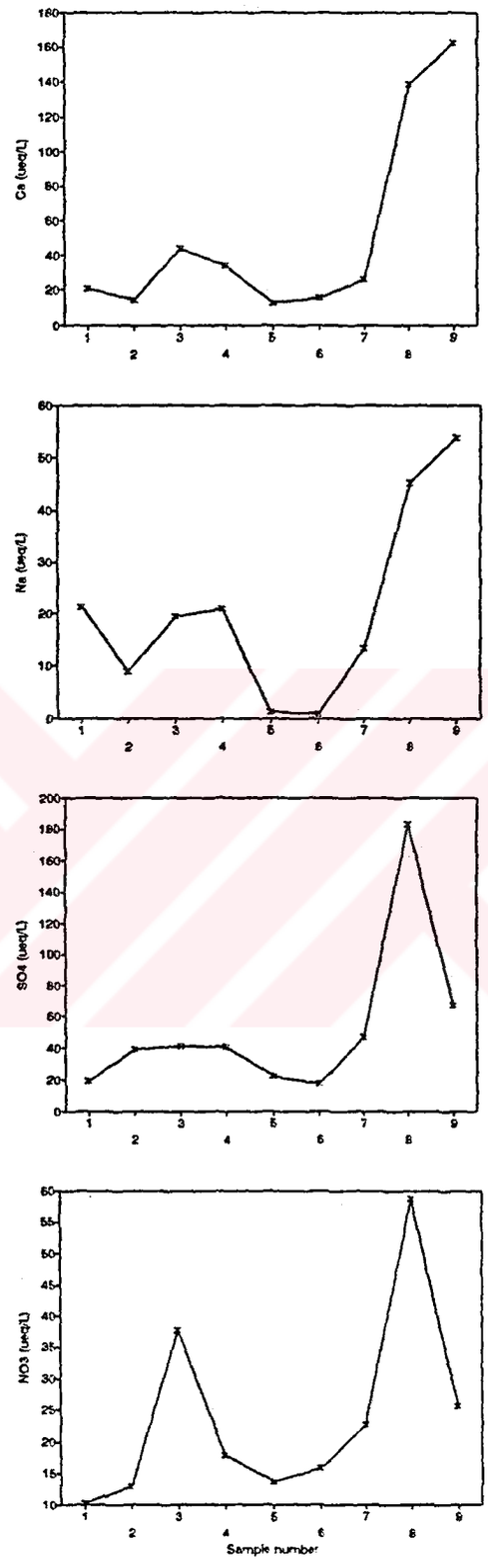

Figure 3.16 Temporal variations of Ca^{2+}, Na^{+}, SO_4^{2-}, NO_3^{-} in snow

except for Mg^{2+} increased in the eighth sample which was taken two weeks later than the previous one. Actually there was snowing between 8^{th} and 9^{th} but it was not taken. In the last sample concentrations again increased and pH of this sample was very high. In general, the longer the precipitation sample remains in the sample container, the longer soil derived particles have to dissolve and reduce the precipitation acidity. This would be expected to be a dominant feature of weekly samples during periods of increased atmospheric particle loading typical of prolonged periods with little precipitation [52].

3.8. Variation in pH

pH change in snow samples is shown in Figure 3.17. Average pH of samples is 4.3 indicating the acidic nature of snow. Samples of 3, 4, 5, 6, 7 were consecutive samples and pH of them increased as snow continued to fall. Same situation was observed for the seventh and eight samples. Eighth sample was taken after two weeks interval and the pH of the sample again decreased since the pollutants were increased in the air during two weeks. Temporal variations of SO_4^{2-}, NO_3^- and pH are shown in the Figure 3.18. Sulfate and nitrate showed the opposite trend with pH. This may indicate large contribution of H_2SO_4 and HNO_3 to H^+ ion concentration. Theoretical calculation of pH was made by assuming the snow solutions were originally made up of the strong acids H_2SO_4 and HNO_3 of atmospheric origin and results are given in the Table 3.13. Nonsea salt sulfate and nitrate concentrations were used

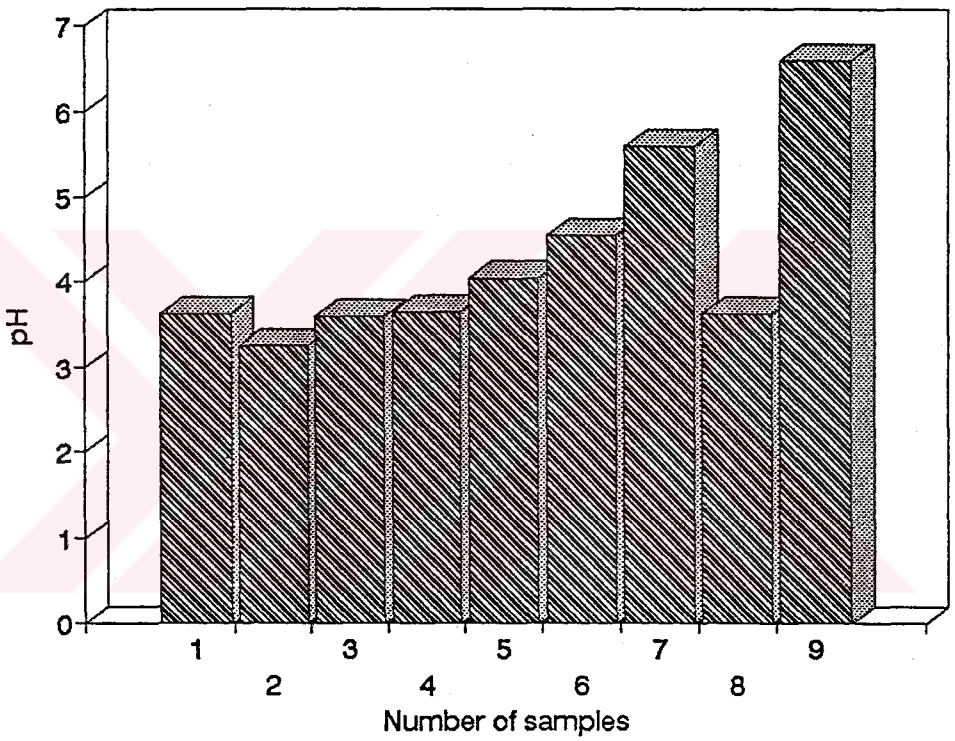

Figure 3.17 pH change in snow samples

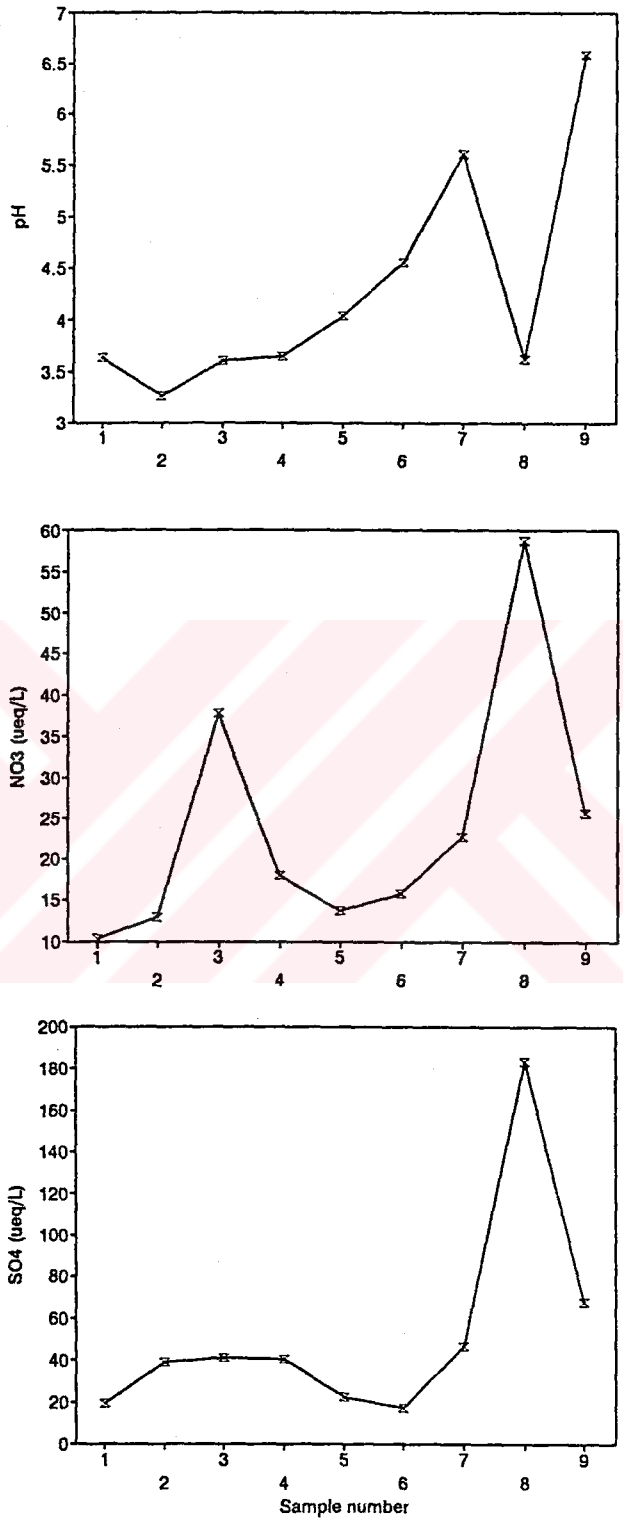

Figure 3.18 Temporal variations of SO_4^{2-}, NO_3 and pH

Table 3.13 Comparison of calculated and measured pH in snow samples.

Sample Number	pH=-Log{2[SO_4^{2-}]$_{nss}$+[NO_3^-]}	Measured pH
1	4.62	3.63
2	4.28	3.26
3	4.13	3.60
4	4.27	3.64
5	4.44	4.04
6	4.48	4.55
7	4.18	5.60
8	3.64	3.62
9	4.10	6.58

in the calculations. Nonsea salt sulfate concentration was calculated by subtracting sea salt contribution of sulfate, assuming all Na concentration came from sea contribution, from total sulfate concentration according to the below formula:

$$[SO_4^{2-}]_{nss} = [SO_4^{2-}]_{total} - \{[Na]_{sample} * [SO_4^{2-}]_{sea}/[Na]_{sea}\}$$

From these calculations it was understood that for the first five samples measured pH was higher than the calculated one. For these five samples also it was found that there was much cation excess. This indicated that organic acids were also important source of acidity. The remaining samples showed relatively good ionic balance. The measured pH was very close to the calculated one for the samples 6 and 8. In other samples measured pH was lower than the calculated ones may be because of the excess basic cations.

3.9. Some Ratios for Snow Samples

Average cation to anion ratio regardless of hydrogen ion concentration was 0.96. When the hydrogen ion concentration was added, the ratio became 3.4. Obvious anion deficiency is possibly due to hydrogen ion associated organic anions that were not analyzed.

Chloride to sodium molar ratio was averaged to be 1.15 (sea water 1.18) indicated marine effect to the sampling site. In aerosol samples Cl was deficient. This suggested that some part of Cl^- concentration was in the gaseous state and scavenged better by snow [47].

Sulfate to nitrate equivalent ratio was 2.1 in snow samples. Other literature values are given in the Table 3.14.

Table 3.14 Comparison of SO_4^{2-}/NO_3^- ratios with literature values.

Ratio	This study	Ref53	Ref21	Ref20	Ref54	Ref17
SO_4^{2-}/NO_3^-	2.1	1.48	0.79	0.96	0.63	0.66

In ref 53, samples were collected on event basis and sampling containers were kept only during snow event in suburban area of city of Montreal. It was found that in winter period, HNO_3 has increased 50 % in importance to H_2SO_4 over 15 years. Long range transport was investigated. However HNO_3 is formed faster than H_2SO_4, that is why HNO_3 is produced locally rather than long range transport. If the air trajectories passed over SO_x and NO_x sources to the west and south-west, pH values were lower and SO_4^{2-} and NO_3^- concentrations were higher in snow. In the rest of the works, winter rain SO_4^{2-}/NO_3^- ratios were compared with snow SO_4^{2-}/NO_3^- ratios. It was seen that this ratio in snow is lower than that in winter rains. In ref 21, samples were collected on event basis with wet-only sampler in urban and rural areas of southeastern Michigan. Snow events were more likely originate from the north with relatively low sulfur emissions. In ref 20, samples were taken daily with wet-only sampler in nine urban areas of northeastern United States. Acidity of snow is increasing more rapidly with nitrate than sulfate suggest that scavenging of gaseous nitric acid is important. Since HNO_3 vapor is scavenged approximately five times faster and five times more efficiently than sulfate and nitrate particles by snow.

In ref 54 samples were taken on event basis using wet-only sampler in suburban area of southeastern Michigan. Lower water content of snow events compared to rain events explain the higher NO_3^- concentrations in snow additionally snow events were from the cleaner northern sector. In ref 17, daily samples were collected by using wet-only sampler in rural area surrounded by deciduous forest at the University of Michigan Biological Station. Nitric acid vapor is scavenged much more efficiently than particulate NO_3^- and accounts for 80-90 % of the snow NO_3^- and air-mass trajectories showed that concentration of HNO_3 was 2-4 times higher in air from south and west. In overall precipitation from south and west accounted for 81 % of the deposited NO_3^-. SO_2 accounted for only 47 % of the total SO_4^{2-} deposited. From these works it is clear that scavenging of HNO_3 vapor, wind direction and precipitation depth are important factors affecting the amount of SO_4^{2-} and NO_3^- in snow. Our study presented that sulfate concentration was much higher than the other values. Higher SO_4^{2-} concentration may be due to two factors firstly high SO_2 emissions with high frequency winds from the southerly directions and its scavenging by snow crystals and secondly from bulky character of snow samples. We don't have any idea about the concentrations of ions in winter rain and the levels of HNO_3 vapor in our sampling site. Thus, acidity of snow mainly came from H_2SO_4 in our sampling site rather than HNO_3.

3.10. Scavenging Ratios and Comparison with Literature Values

Scavenging ratio relates airborne concentration to snow composition. Scavenging ratio was calculated by taking the ratio of the concentration of the ion in snow to the concentration of the same ion in air measured simultaneosly and multiplied by the density of air to make the ratio a dimensionless quantity as it is described in the section 1.4.1. Scavenging ratio shows the cleaning capacity of snow. Scavenging ratios of ions are tabulated together with the literature values in the Table 3.15. Of course snow scavenges the gaseous pollutants together with particulates. Therefore calculated sulfate and nitrate ratios included SO_2 and HNO_3 scavengings respectively. Scavenging values of sulfate greater than 500 was probably caused by SO_2 scavenging during snow events [17]. Variation in ratios can also be attributed to differences in particle size, with the smallest particles having the lowest ratio. It was expected to have high scavenging ratio for Ca^{2+} as it is associated with large particles because of its dominant crustal source, however in our work it was seen that calcium scavenging ratio was not high. Ammonium had the lowest ratio as it was expected since it is usually found on small particles. Magnesium had the highest ratio. Although scavenging ratio of chloride is less than the other work, it has a significant high ratio value due to the high concentration of chloride in the gaseous phase. However concentrations in snow were not free of dry deposition.

Table 3.15 Comparison of scavenging ratios with literature values.

Ions	This work		Ref 17		Ref 22
	Scavenging Ratio	Range	Scavenging Ratio	Range	Scavenging Ratio
Cl^-	950	88-1025			3200
NO_3^-	650	95-2780	1000		940
SO_4^{2-}	630	60-1630	570	60-2280	350
NH_4^+	180	10-340	410	40-2200	300
Mg^{2+}	2000	240-7060			
Na^+	675	17- 2400			
K^+	705	350-1060	1000		
Ca^{2+}	310	25-960	2600	170-8190	

3.11. Correlation of Ions

Ion pair correlation coefficients are shown in the Table 3.16. The highest correlation coefficients appear for the ion pairs Na and Cl (r=0.90), Ca and Cl(r=0.92), NO_3 and SO_4(r=0.88), NH_4 and NO_3(r=0.94), NH_4 and SO_4(r=0.93), Ca and Na(r=0.94). Most of these well correlated pairs have common sources or occur in snow as a result of a common source or compound for example NaCl, $CaCl_2$, NH_4NO_3, $(NH_4)_2SO_4$, $CaSO_4$ etc. Calcium, K and Na are also correlated well. This suggest that they have soil and seasalt aerosols. The relatively high correlations of NH_4^+ and NO_3^- and NH_4^+ and SO_4^{2-} results from the reaction of sulfuric and nitric acids with gaseous NH_3. Likewise, the correlations of Ca^{2+} with SO_4^{2-} and NO_3^- may be the result from the reaction of these acids with alkaline compounds containing Ca^{2+}. Good

correlation between SO_4^{2-} and NO_3^- is probably due to the coemission of their direct precursors SO_2 and NO_x from fossil fuel combustion. These results are supported further by anion versus cation combination. The correlation coefficient for $(SO_4^{2-}+NO_3^-)$ versus $(Ca^{2+}+Mg^{2+}+NH_4^+)$ is 0.83 and average anion to cation equivalent ratio is 1.1. This very high anion to cation correlation indicates again that the major part of SO_4^{2-} and NO_3^- in snow is associated with NH_4^+,Ca^{2+}, Mg^{2+} ions.

Table 3.16 Binary correlation coefficients between ions in snow.

	H^+	Cl^-	NO_3^-	SO_4^{2-}	Mg^{2+}	Na^+	K^+	Ca^{2+}	NH_4^+
H^+	1.00								
Cl^-	-0.43	1.00							
NO_3^-	-0.00	-0.43	1.00						
SO_4^{2-}	0.085	0.64	0.88	1.00					
Mg^{2+}	-0.48	0.23	0.25	0.27	1.00				
Na^+	-0.11	0.90	0.61	0.69	0.43	1.00			
K^+	-0.32	0.73	0.69	0.45	-0.035	0.64	1.00		
Ca^{2+}	-0.22	0.92	0.67	0.75	0.41	0.94	0.64	1.00	
NH_4^+	0.63	0.58	0.94	0.93	-0.05	0.66	0.56	0.66	1.00

CHAPTER IV

CONCLUSIONS

Concentrations of major ions in aerosol and snow samples in Uludağ Mountain were determined in this work. In aerosol samples sulfate and calcium had the highest concentrations. Calcium , magnesium, sodium and potassium were originated from mostly crustal contribution since they had high concentrations in dry season. However magnesium and sodium were also affected by sea salt contribution and so they had high coefficient of variation. Maximum concentration of sulfate and nitrate were observed during winter and spring respectively. Chloride had the highest concentration in November and December. These high concentrations were associated with northerly winds which carries marine aerosols from Marmara Sea to our station. The average Cl^- to Na^+ ratio (0.9) dropped to a value as low as 0.4 during autumn as a result of larger crustal sodium concentration during this season. Ammonium had its highest concentration in autumn and spring seasons which are the fertilizing seasons in agricultural areas. Calculation of base-line concentrations showed that they represented the regional background concentrations and concentrations of Cl^-, Ca^{2+}, NO_3^-, SO_4^{2-} and NH_4^+ were mostly affected by the anthropogenic sources.

High concentrations of both SO_2 to SO_4^{2-} were observed during winter. Considering low rate of conversion of SO_2 to SO_4^{2-}, observed results implied the long range transport of sulfate in wintertime.

Dominating winds in the sampling site are from S, SSW, SSE directions, with a frequency of 80 % of sampling period. Wind sector analyses revealed three main pollution sources namely urban and industrial areas, ski resort area and power plant. The sources located at north had the same pollution strength as the sources located at south, but southerly winds made the greatest contribution to all parameters because of high frequency of winds from this sector. The northerly winds carries the plumes of urban and industrial emissions and marine aerosol to our sampling site and southerly winds carries the plume of a power plant and ski resort area.

Potassium, Mg^{2+}, NH_4^+, Cl^-, NO_3^- and SO_4^{2-} had the highest average concentrations from the north sectors. Southerly winds (SSE, S, SSW) made the percent contributions of 90 % for Mg^{2+}, 89 % for K^+, 86 % for NH_4^+, 88 % for Cl^-, 94 % for NO_3^- and 88 % for SO_4^{2-}. Chloride originated from the Marmara Sea which is at the north of the station. Agricultural areas which are located at NNE direction controlled the concentration of NH_4^+. Higher SO_4^{2-} and NO_3^- concentrations were partly the result of the long range transport from the north. The effect of the power plant was found to be very dominant for SO_2 and TSP.

Anion deficiency of anions was observed in ion balance calculations of both aerosol and snow samples. Organic acids were responsible for anion deficiency. Organics were also responsible for avoiding acids to be neutralized by basic cations, especially in aerosols.

Scavenging power of snow were comparable with literature values. The most strongly scavenged ion was magnesium in snow.

CHAPTER V

RECOMMENDATIONS FOR FUTURE WORK

In the previous study [55] concerning the gaseous pollutant measurements in Uludağ National Park, obtained concentrations and meteorological data were interpreted to explain the reasons of the severe damage of pollution to pine forest in Uludağ. But, it was not complete data in order to explain the chemical composition of the ambient atmosphere in the sense that only gas phase pollutants and total suspended matter were measured. Therefore it was partly completed with the aerosol and wet deposition data with this work. It was partly because these additions were the preliminary steps of future advanced works. In the future it is recommended that the sampling of aerosol should be done in longer period (at least a year) and size fractionated form and analysis of them should include trace metals and major organic anions such as formate and acetate ions which are found to be very important ions in forested area for source apportionment. In addition to these, bulk snow sampling may be switched to event sampling by using wet only sampler to obtain pure wet deposition data without the contamination of dry deposition. Likewise aerosol, the analysis of snow samples should involve trace metals and organic anions as well as the major ions. Sampling period should be at least one or more years. In this way a large and a complete data set is

obtained for sophisticated statistical methods. One can obtain quantitative and qualitative information about specific sources or class of sources applying factor analysis or chemical mass balances. Long range pollution transport can also be investigated using upper air meteorological data.

REFERENCES

[1] Finlayson-Pitts B. and Pitts J. N. (1986). *Atmospheric Chemistry: Fundamentals and Experimental Techniques*, Wiley-Interscience publication, New York, USA, p: 13, 47, 737-739.

[2] Clarke A. G. (1986). *The air, Understanding Our Environment*, ed: Hester R. E., The Royal Society of Chemistry Bristol, England, p: 71-104.

[3] Faust Bruce C. (1994). Photochemistry of clouds, fogs, and aerosols. *Environmental Science and Technology* **28**, 217A-222A.

[4] Perkins H. C. (1974). *Air Pollution*, Mc. Graw-Hill, Inc. printed in New York USA, p: 4-5.

[5] Apsimon H. M., Kruse M. and Bell J. N. B. (1987). Ammonia emissions and their role in acid deposition. *Atmospheric Environment* **21**, 1939-1946.

[6] Daum P. H., Kelly T. J., Tanner R. L. and Tang X. (1989). Winter measurements of trace gas and aerosol composition at a rural site in southern Ontario. *Atmospheric Environment* **23**, 161-173.

[7] Fung C. S., Misra P. K., Bloxam R. and Wong S. (1991). A numerical experiment on the relative importance of H_2O_2 and O_3 in aqueous conversion of SO_2 to SO_4^{2-}. *Atmospheric Environment* **25A**, 411-423.

[8] Bricker O.P. and Rice K. C. (1993). Acid rain. *Annu. Rev. Earth Planet. Sci.* **21**, 151-174.

[9] Eder B. K. and Dennis R. L. (1990). On the use of scavenging ratios for the inference of surface-level concentrations and subsequent dry deposition of Ca^{2+}, Mg^{2+}, Na^+ and K^+. *Water, Air, and Soil Pollution* **52**, 197-216.

[10] Rao P. S. P., Khemani L. T., Momin G. A., Safai P. D. and Pillai A. G. (1992). Measurements of wet and dry deposition at an urban location in India. *Atmospheric Environment* **26B**, 73-78.

[11] Schultz Judith A. Meyer (1994). Urban wet deposition nitrate: A comparison to non-urban deposition. *Water, Air, and Soil Pollution* **73**, 83-93.

[12] Schumann Thomas (1991). Aerosol and hydrometeor concentrations and their chemical composition during winter precipitation along a mountain slope- III. Size-differentiated in-cloud scavenging efficiencies. *Atmospheric Environment* **25A**, 809-824.

[13] Barrie L. A. and Schemenauer R. S. (1986). Pollutant wet deposition mechanism in precipitation and fog water. *Water, Air and Soil pollution* **30**, 91-104.

[14] United Nations Environment Programme (UNEP) and the Secretariat of the United Nations Economic Council for Europe (1991), Interm report on cause-effect relationships in forest decline . *Global Environment Monitoring System , p: 7-91.*

[15] Mitra S. K., Barth U. and Pruppacher H. R. (1990). A laboratory study of the efficiency with which aerosol particles are scavenged by snow flakes. *Atmospheric Environment* **24A**, 1247-1254.

[16] Davidson I. C., Honrath R. E., Kadane J. B., Tsay R. S, Mayewski P. A., Lyons W. B., and Heidam N. Z. (1987). The scavenging of atmospheric sulfate by Arctic snow. *Atmospheric Environment* **21**, 871-882.

[17] Cadle S.H., Kopple R. V., Mulawa P. A. and Dasch J. M. (1990). Ambient cencentrations, scavenging ratios, and source regions of acid related dompounds and trace metals during winter in Northern Michigan. *Atmospheric Environment* **24A**, 2981-2989.

[18] Chan Walter H. and Chung David H. S. (1986). Regional-scale precipitation scavenging of SO_2, SO_4, NO_3 and HNO_3. *Atmospheric Environment* **20**, 1397-1402.

[19] Dasch J. M. (1987). On the difference between SO_4^{2-} and NO_3^- in wintertime precipitation. *Atmospheric Environment* **21**, 137-141.

[20] Topol E. L. (1986). Differences in ionic composition and behavior in winter rain and snow. *Atmospheric Environment* **20**, 347-355.

[21] Dasch J. M. and Cadle S. H. (1985). Wet and dry deposition monitoring in southeastern Michigan. *Atmospheric Environmnet* **19**, 789-796.

[22] Baltensperger U., Schwikowski M., Gaggeler H. W., Jost D. T., Beer J., Siegenthaler U., Wagenbach D., Hofmann H. J. and Synal H. A. (1993). Transfer of atmospheric constituents into an Alpine snow field. *Atmospheric Environment* **27A**, 1881-1890.

[23] Bell D. A. and Clive P. R. Saunders (1991). The scavenging of high altitude aerosols by small ice crystals. *Atmospheric Environment* **25A**, 801-808.

[24] National Research Concil of Canada (1982). *Effects of aerosols on atmospheric processes*, publications NRCC/CNRC in Canada, p:172-174.

[25] Duncan C. L., Welch B. E., Ausserer W. (1986). The compositin of precipitation at Snoqualmie Pass and Stevens Pass in the Central Cascades of Washington State. *Water, Air and Soil Pollution* **30**, 217-229.

[26] Duncan C. L. (1992). Chemistry of rime and snow collected at a site in the Central Washington. *Environ. Sci. Tech.* **26**, 61-66.

[27] McBean G. A. and Nikleva S. (1986). Composition of snow in Pacific Coastal Mountains. *Atmospheric Environment* **20**, 1161-1164.

[28] Davies T.D., Tranter M., Jickells T. D., Abrahams P. W., Landsberger S., Jarvis K. and Pierce C. E. (1992). Heavily-contaminated snowfalls in the remote Scottish Highlands: A consequence of regional scale mixing and transport. *Atmospheric Environment* **26A**, 95-112.

[29] Mahadevan T. N., Negi B. S. and Meenakshy V. (1989). Measurement of elemental composition of aerosol matter and precipitation from a remote background site in India. *Atmospheric Environment* **23**, 869-874.

[30] Sopauskiene D. and Budvytyte D. (1994). Chemical characteristics of atmospheric aerosol in rural site of Lithuania. *Atmospheric Environment* **28**, 1291-1296.

[31] Wake C. P., Dibb J. E. and Mayewski P. A. (1994). The chemical composition of aerosols over the Eastern Himalayas and Tibetan plateau during low dust periods. *Atmospheric Environment* **28**, 695-704.

[32] Ungör S. (1992). Ion Chemistry in Ankara Atmosphere. *Master Thesis in Chemistry Department*, METU, Ankara.

[33] Frankenberger W. T., Mehra H. C. and Gjerde D. T. (1990). Environmental application of ion chromatography. *Journal of Chromatography* **504**, 211-245.

[34] Standard test methods for ammonia nitrogen in water. (1979). *ASTM* **D 1426-79.**

[35] Pio C. A., Santos I. M., Anacleto T. D. and Nunes T. V. (1991). Particulate and gaseous air pollutant levels at the Portuguese west coast. *Atmospheric Environment* **25A**, 669-680.

[36] Hacısalihoğlu G., Balkaş T. I., Tuncel S. G., Herman D. H., Ölmez I. and Tuncel G. (1991). Trace element composition of the Black Sea aerosols. *Deep-Sea Research* **38**, 1255-1266.

[37] Güllü G. and Tuncel G. (1995). Unpublished data.

[38] Kitto A. N., Harrison R. M. (1992). Processes affecting concentrations of aerosol strong acidity at sites in Eastern England. *Atmospheric Environment* **26A**, 2389-2399.

[39] Brewer P. G. (1975). *Minor Elements in sea water,* ed: Chester R. Chemical oceanography, Vol 1., Academic press, New York, p: 417-425.

[40] Legrand M. R. and Delmas R. J. (1984). The ionic balance of Antarctic snow: A 10-year detailed records. *Atmospheric Environment* **18**, 1867-1874.

[41] Fung C. S., Mısra P. K., Bloxam R. and Wong S. (1991). A numerical experiment on the relative importance of H_2O_2 and O_3 in aqueous conversion of SO_2 to SO_4^{2-}. *Atmospheric Environment* **25A**, 411-423.

[42] Anlauf K. G., Bottenheim J. W., Brice K. A. and Wiebe H. A. (1986). A comparison of summer and winter measurements of

atmospheric nitrogen and sulphur compounds. *Water, Air and Soil Pollution* **30**, 153-160.

[43] Hilst G. R. (1992). Proportionality between SO_2 emissions and wet SO_4^{2-} concentrations the effect of area of averaging. *Atmospheric Environment* **26A**, 1413-1420.

[44] Keene W. C., Galloway J. N. and Holden J. D. (1983). Measurement of weak organic acidity in precipitation from remote areas of the world. *Journal of Geophysical Research* **88**, 5122-5130.

[45] Guiang S. F., Krupa S. V. and Pratt G. C. (1984). Measurement of S(IV) and organic anions in Minnessota Rain. *Atmospheric Environment* **18**, 1677-1682.

[46] Yamaguchi K., Tatano T., Tanaka F., Nakao M., Gomyoda M. and Hara H. (1991). An analysis of precipitation chemistry measurements in Shimane, Japan. *Atmospheric Environment* **25A**, 285-291.

[47] Harriss R. C., Wofsy S. C., Garstang M., Browell E. V., Molion L. C. B., Mcneal R. J., Hoell J. M., Bendura R. J., Beck S. M., Navarro R. L., Riley J. T. and Snell R. L. (1988). The Amazon Boundary layer experiment (ABLE 2A): Dry season 1985. *Journal of Geophysical Research* **93**, 1351-1360.

[48] Yatın M. (1994). Source apportionment of urban aerosols using receptor modelling approach: An application to Ankara. *Ph. D. Thesis in Chemistry Department*, METU, Ankara.

[49] Vossler T. L., Lewis C. W., Stevens R. K., Gordon G. E., Tuncel S. G., Russwurm G. M. and Keeler G. J. (1989). Composition and origin of summertime air pollutants at deep creek lake, Maryland. *Atmospheric Environment* **23**, 1535-1547.

[50] Reynolds B. (1983). Techical Note, The chemical composition of snow at a rural upland site in Mid-Wales. *Atmospheric Environment* **17**, 1849-1851.

[51] Berg N., Dunn P., Fenn M. (1991). Spatial and temporal variability of rime ice and snow chemistry at five sites in California. *Atmospheric Environment* **25A**, 915-926.

[52] Sisterson D. L., Wurfel B. E. and Lesht B. M. (1985). Chemical differences between event and weekly precipitation samples in northeastern Illinois. *Atmospheric Environment* **19**, 1453-1469.

[53] Lewis E. J., Moore T. R., Enright N. J. (1983). Spatial-temporal variations in the Montreal region. *Water, Air and Soil Pollution* **20**, 7-22.

[54] Dasch J. M. (1987). On the difference between SO_4^{2-} and NO_3^- in wintertime precipitation. *Atmospheric Environment* **21**, 137-141.

[55] Baykal A. (1994). Measurement and source determination of air pollutants in Uludağ National Park. *Master Thesis in Chemistry Department*, METU, Ankara.

APPENDIX

DAILY CONCENTRATIONS OF IONS IN AEROSOL SAMPLES

	IONS (ug/m3)							
DAYS	Cl	NO3	SO4	NH4	Mg	Na	K	Ca
SEPTEMBER(1993)								
2		0.217	0.450	0.651	0.030	0.466	0.044	
3		0.386	2.192		0.053	0.542	0.085	0.381
4	0.117	0.589	3.308	2.004				
5	0.103	0.361	1.992	2.598	0.079	0.716	0.066	0.140
6	0.114	0.453	2.403	3.072	0.092	0.645	0.108	0.477
7	0.142	0.367	2.019	1.862	0.052	0.407	0.108	0.324
8	0.286	0.472	1.772	3.072	0.207	1.224	0.093	0.960
9	0.325	0.444	1.822	1.173	0.095	0.782	0.098	1.203
10				1.458	0.648	4.525	0.059	5.715
11		1.411	0.458	0.770	0.057	0.625	0.044	0.203
12	0.144	1.167	1.703	2.789	0.216	1.278	0.094	2.449
13				2.029	0.277	0.840	0.125	2.245
14		0.911	2.233	3.025	0.184	1.224	0.111	1.782
15	0.519	1.067	3.450	3.311	0.227	0.970	0.136	2.037
16		1.939	5.897	3.478	0.426	1.072	0.145	3.319
17	0.097	1.353	5.083	1.529	0.231	0.544	0.128	1.550
18	0.153	2.658	5.139	4.331	0.441	1.452	0.147	3.642
19	0.203	1.597	3.461	1.601	0.528	1.678	0.106	3.155
20	0.183	0.692	4.844	1.720				
21	0.347	0.664	2.694	1.244	0.252	1.308	0.084	0.358
22	0.311	1.419	1.931	2.050	0.105	0.948	0.083	0.477
23	0.103	0.464	0.639	0.746	0.120	0.417	0.064	0.294
24	0.083	0.186	2.517	1.957	0.195	1.245	0.101	1.296
25		0.844	1.569	0.746	0.177	0.535	0.077	0.572
26		0.739	1.622	1.292	0.185	0.629	0.127	1.251
27	0.122	0.583	3.322	1.149	0.195	0.477	0.164	1.559
28	0.294	1.436	3.308	1.791	0.059	1.072	0.212	4.243
29	0.244	1.047	4.822	2.123	0.255	1.242	0.225	1.743
30	0.175	0.553	1.508	0.818	0.084	0.560	0.084	0.558

OCTOBER	Cl	NO3	SO4	NH4	Mg	Na	K	Ca
1	0.264	0.475	1.192	0.268	0.061	0.818	0.118	1.107
2	0.264	0.808	1.728		0.683	3.479	0.056	5.654
3	0.033	0.503	2.206	0.268	0.561	6.461	0.081	4.818
4	0.033	0.436	1.567		0.400	1.117	0.066	2.931
5	0.561	1.022	1.992	0.700			0.161	
6	0.211	0.389		0.483	0.140	0.690	0.045	0.301
7	0.033	0.328	1.297		0.103	0.185	0.049	0.394
8	0.317	0.011	0.947	1.303	0.447	3.465	0.045	3.146
9	0.033	0.578	0.878		0.169	0.587	0.065	1.554
10	0.350	0.872	2.389	0.203	2.492	11.738	0.078	
11	0.831	0.633	1.364		0.189	0.582	0.066	1.527
12				0.547	0.228	0.970	0.109	2.320
13	0.033	0.783	2.389		0.168	0.475	0.065	1.267
14	0.242	0.011	3.450	1.022	0.355	1.261	0.128	3.198
15	0.033	0.561	2.553	0.246	0.197	0.462	0.083	1.694
16	0.283	0.647	0.892	0.829	0.169	0.420	0.059	1.328
17	0.353	0.847	2.203		0.209	0.398	0.107	2.866
18	0.261	0.550	0.781		0.105	0.308	0.065	0.909
19	0.278	0.881	0.983	0.829	0.319	0.962	0.093	3.407
20	0.214	0.675	0.764		0.180	0.585	0.085	2.088
21	0.228	0.864	0.986		0.186	0.890	0.083	2.328
22	0.033	0.406	1.381		0.394	1.237	0.092	2.580
23	0.292	1.053	2.194	1.023	0.291	1.602	0.118	3.698
24	0.306	1.144	3.261	0.700	0.199	0.946	0.119	2.538
25	0.292	1.053	2.083	1.110	1.035	5.451	0.107	
26	0.219	1.533	5.544	0.656	0.289	0.979	0.133	2.380
27	0.033	1.233	5.314	1.282	0.117	0.786	0.101	1.021
28	0.033	0.247	1.975		0.040	0.377	0.058	0.010
29	1.506	0.378	2.428		0.063	0.424	0.084	0.230
30	1.164	0.439	3.089		0.087	1.154	0.122	0.446
31	2.489	0.511	3.992		0.106	0.608	0.141	0.492
NOVEMBER								
1				0.568	0.066	0.783	0.078	0.090
2	1.742	0.286	2.189	1.731	0.058	0.425	0.075	0.147
3	1.689	0.161	3.011	1.928	0.130	0.770	0.087	0.551
4	0.047	0.164	1.197	0.913	0.105	0.576	0.095	1.363
5	0.214		1.567	0.337	0.167	1.104	0.122	0.547
6	1.689	0.647	1.811	0.939	0.143	0.539	0.120	0.737
7	0.953	0.406	3.392	1.088	0.205	0.872	0.118	
8	2.622	2.444	13.342	1.347	0.208	0.815	0.148	
9	1.261	1.119	4.031	1.106	0.087	0.820	0.092	
10	2.364	0.203	0.922	0.509	0.052	0.707	0.052	0.218

DECEMBER	Cl	NO3	SO4	NH4	Mg	Na	K	Ca
7	3.869	0.744	12.853	2.106	0.044	0.447	0.097	
8	1.722	0.283	3.650		0.010	0.982	0.087	
9	2.350	3.319	7.000		0.093	1.077	0.097	1.726
10	0.125	0.308	1.486	1.726	0.057	0.389	0.048	0.191
11	2.056	1.878	11.897	2.004	0.048	0.829	0.081	
12	0.175	0.067	0.886	0.551	0.030	0.431	0.068	
13	1.661	0.203	1.500	0.809	0.023	1.891	0.047	
14	1.247		0.383	1.317	0.031	0.646	0.055	0.059
15	2.169	0.858	2.278		0.088	0.994	0.055	
16	0.631	0.547	4.356	1.282	0.079	0.630	0.066	
17				0.431	0.073	0.801	0.070	
19	1.100	0.058	0.339	2.528	0.040	0.394	0.030	0.364
20	1.128	0.086	0.236	0.224	0.003	0.124	0.025	
21	0.186	0.211	1.158	0.076	0.053	0.576	0.081	
22	1.975	0.297	5.153		0.035	0.447	0.063	
23		0.053	1.256	0.589	0.034	1.194	0.073	
24	0.869	0.475	4.681	0.795	0.127	1.269	0.133	0.018
JANUARY (1994)								
12	0.169	1.192	0.792	0.679	0.058	0.394	0.043	0.018
13	0.142	0.367	1.172	0.598	0.043	0.293	0.043	
14	0.203	0.539	1.714	0.672	0.100	0.366	0.079	4.073
15	0.022	0.119	0.869	0.466	0.126	0.051	0.043	6.627
16	0.281	0.303	1.950	1.072	0.191	0.221	0.070	7.401
17	0.967	0.392	1.375	0.478	0.097	0.505	0.056	
18	0.181	0.267	1.286	0.647	0.240	0.450	0.079	8.669
19	0.217	0.369	1.511	1.214	0.205	0.488	0.079	7.672
20	0.333	0.133	0.714	0.711	0.132	0.091	0.061	7.053
21	0.214	0.094	0.319	0.311	0.196	0.041	0.056	8.969
22		0.069	0.322	0.400	0.058	0.133	0.029	0.560
23					0.021		0.001	0.821
24	0.114	0.044	0.053	0.598	0.056	0.112	0.011	2.273
25	0.197	0.100	0.125	0.221	0.108	0.005	0.024	5.098
26	0.853	0.281	0.492	0.375	0.132	0.188	0.052	5.524
27	0.003	0.228	0.928	0.619	0.143	0.171	0.070	5.708
28				0.090	0.167	0.280	0.079	5.534
29		0.100	0.208	0.246	0.121	0.055	0.029	5.147
30	0.003	0.106	0.406	0.221	0.115	0.097	0.034	5.069
31	0.197	4.464	1.303		0.115	0.209	0.066	4.876

FEBRUARY	Cl	NO3	SO4	NH4	Mg	Na	K	Ca
1		0.458	1.019		0.069	0.280	0.052	
2		0.072	0.275		0.065	0.158	0.020	
3	0.031	0.358	1.325	0.131	0.060	0.471	0.056	
4		0.147	0.950	0.129	0.065	0.184	0.034	
5	1.764	0.414	3.700	0.233	0.084	0.333	0.052	
6					0.067	0.255	0.052	
7	0.153	0.608	1.753	1.458	0.071	0.314	0.042	
8	0.244	0.728	4.761		0.100	0.469	0.089	
9	0.158	0.456	2.961	0.168	0.086	0.345	0.061	
10	0.299	4.381	3.412		0.040	0.371	0.106	0.579
11	0.198	2.721	1.776		0.011	0.055	0.036	0.571
12	0.121	2.074	1.126		0.016	0.242	0.057	0.421
13	0.206	2.802	1.259		0.002	0.045	0.019	0.442
14	0.251	2.629	1.436		0.010	0.217	0.079	0.339
15	0.299	0.456	1.053		0.008	0.079	0.033	0.367
16	0.511	0.820	1.803	0.203	0.031	0.255	0.015	
17	0.136	0.356	0.358	0.022	0.004			0.028
18	0.136	0.325	0.403	0.142	0.001	0.033	0.003	
19	0.330	0.619	1.653	0.022	0.035	0.320	0.026	0.033
20	0.411	0.507	1.778	0.061	0.051	0.446	0.002	0.041
21	0.194	0.408	1.936		0.006	0.068	0.030	
22	0.183	0.411	3.259	0.364	0.011	0.194	0.032	
23	0.283	0.338	2.367	0.142	0.004	0.062	0.025	0.958
24	0.209	0.407	2.405	0.486	0.003	0.087	0.022	0.619
25	0.250	0.219	0.351	1.514	0.003	0.263	0.021	
26	0.205	0.264	4.621	1.414	0.016	0.120	0.045	0.146
27	0.209	0.330	1.112	1.131	0.012		0.014	0.639
28	0.118		0.447	0.706	0.017	0.025		0.878
MARCH								
1	0.237	8.430	0.787	0.847	0.026		0.012	
2	0.126	1.437	1.637	0.244	0.037	0.182	0.036	0.889
3				0.989	0.057	0.135	0.039	1.196
4				0.303	0.013	0.087	0.017	0.613
5				0.081	0.018	0.072	0.064	0.529
6	0.253	0.621	1.027	0.061	0.026	0.009	0.014	0.856
7	0.177	0.269	3.979	0.747	0.012	0.119	0.042	0.373
8	0.357	1.107	3.157	1.192	0.013	0.208	0.051	0.448
9	0.280	1.279	4.791	2.281	0.007	0.180	0.042	0.349
10	0.506	1.356	3.131	2.725	0.006	0.267	0.045	0.217

MARCH	Cl	NO3	SO4	NH4	Mg	Na	K	Ca
11		1.069	2.003	1.656	0.003	0.174	0.051	0.384
12	0.407	1.335	1.951	1.817	0.017	0.245	0.034	0.585
13	0.140	1.058	1.861	1.089	0.015	0.138	0.049	0.529
14	0.127	0.886	0.171	0.283	0.004	0.077	0.001	0.414
15	0.202	1.190	0.926	0.847	0.001	0.096	0.016	0.218
16	0.628	1.600	1.022	1.556	0.022	0.320	0.041	0.488
17	0.253	0.994	0.299	0.061	0.001	0.057	0.010	0.467
18	0.209	2.747	0.258	0.322	0.020	0.191	0.011	0.754
19	0.176	1.530	1.571	1.633	0.030	0.381	0.038	0.691
20			0.863	0.486	0.045	0.286	0.026	0.895
21	0.204	3.650	2.249	0.847	0.039	0.279	0.045	0.601
22	0.119	1.340	2.425	1.817	0.047	0.398	0.035	0.611
23	0.130	1.025	1.034	0.989	0.010	0.080	0.016	0.674
24	0.247	1.590	0.123	0.103	0.015	0.091	0.010	0.648
25	0.306	2.993	3.325	0.344	0.017	0.127	0.035	0.769
26	0.122	5.863	0.995	1.797	0.044	0.415	0.094	1.234
27	0.263	1.220	1.897	0.264	0.029	0.215	0.016	0.713
28	0.161	1.417	3.610	1.533	0.046	0.355	0.052	0.923
29	0.165	1.413	4.583	1.575	0.033	0.381	0.052	0.744
30	0.380	1.197	1.354	0.564	0.045	0.257	0.019	1.180
31	0.291	1.167	0.546	0.103	0.012	0.221	0.021	0.440
APRIL								
1	0.305	0.965	0.798	0.042			0.003	
2	0.281	1.160	0.514		0.008	0.046		0.413
3	0.339	1.039	0.389	0.860	0.006	0.064	0.004	0.348
6	0.655	0.761	0.111	0.122	0.068	0.026	0.008	1.317
7	0.306	0.719	0.684	0.203	0.032	0.052	0.009	1.048
8	0.440	1.371	2.520	1.694	0.021	0.251	0.027	0.802
9	0.308	1.180	4.141	2.825	0.030	0.354	0.055	0.519
10	0.383	0.943	0.504	0.486	0.009	0.117	0.004	0.562
11	0.389	1.037	2.049	1.069	0.011	0.190	0.015	0.599
12	0.341	0.950	1.498	0.969	0.008	0.168	0.011	0.286
13	0.240	1.411	0.560	0.283	0.003			0.381
14	0.581	0.829	0.501	0.264	0.007		0.001	0.411
15	0.106		3.172	1.675	0.041	0.376	0.058	0.785
16	0.389	2.290	3.296	1.575	0.049	0.409	0.050	0.886
22	0.417	8.757	3.504	1.625	0.045	0.372	0.055	0.844
23	0.685	0.911	2.050	0.606	0.151	0.727	0.062	2.822
24	0.707	1.644	0.637	0.322	0.061	0.346	0.009	0.847
25	0.347	1.579	0.982	0.303	0.013	0.063	0.005	0.436